

# Quantum Reading of a Classical Memory

Stefano Pirandola

Department of Computer Science, University of York, York YO10 5DD, United Kingdom

(Dated: January 11, 2019)

We consider a simple model of digital memory where each cell is a reflecting medium with two possible reflectivities (used to store a bit of information). Adopting this model, we show that a non-classical source of light, possessing Einstein-Podolsky-Rosen correlations, can retrieve more information than any classical source. This improvement is shown in the regime of high reflectivities and few photons, where the gain of information can be dramatic. As a result, quantum light can be used to increase storage capacities and data-transfer rates of classical digital memories.

PACS numbers: 03.67.-a, 03.65.-w, 42.50.-p

In recent years, non-classical states of radiation have been exploited to achieve marvellous results in quantum information and computation [1, 2]. In the language of quantum optics, the bosonic states of the electromagnetic field are called “classical” when they can be expressed as probabilistic mixtures of coherent states. Classical states describe practically all the radiation sources which are used in today’s technological applications. By contrast, a bosonic state is called “non-classical” when its decomposition in coherent states is non-positive [3, 4]. One of the key properties which makes a state non-classical is the quantum entanglement. In the bosonic framework, this is usually present under the form of Einstein-Podolsky-Rosen (EPR) correlations [5], meaning that the position and momentum quadrature operators of two bosonic modes are so correlated to beat the standard quantum limit [6]. This is a well-known feature of the two-mode squeezed vacuum (TMSV) state [2], one of the most important states routinely produced in today quantum optics’ labs.

In this Letter, we show how the use of non-classical light possessing EPR correlations can *widely* improve the readout of information from classical digital memories. To our knowledge, this is the first study which proves and quantifies the advantages of using non-classical light for this fundamental task, being absolutely non-trivial to identify the physical conditions that can effectively disclose these advantages (as an example, see the recent no-go theorems of Ref. [7] applied to quantum illumination [8–11]). Our model of digital memory is simple but can potentially be extended to realistic optical disks, like CDs and DVDs, or other kinds of memories, like the barcodes. In fact, we consider a memory where each cell is composed by a reflecting medium with two possible reflectivities,  $r_0$  and  $r_1$ , used to store a bit of information. This memory is irradiated by a source of light which is able to resolve every single cell. The light focussed on, and reflected from, a single cell is then measured by a detector, whose outcome provides the value of the bit stored in that cell. Besides the “signal” modes irradiating the target cell, we also consider the possible presence of ancillary “idler” modes which are directly sent to the detector. The general aim of these modes is to improve the performance of the output measurement by exploit-

ing possible correlations with the signals. Adopting this model and fixing the number of photons irradiated over the memory, we show that a *non-classical* source of light with EPR correlations between signals and idlers can retrieve more information than any classical source of light. In particular, this is proven for high reflectivities (typical of optical disks) and few photons irradiated. In this regime the difference of information can be surprising, i.e., up to 1 bit per cell (corresponding to the extreme situation where only quantum light can retrieve information). As we will discuss in the conclusion, the chance of reading digital memories using few photons leads to remarkable consequences, like boosting their storage capacities and data-transfer rates.

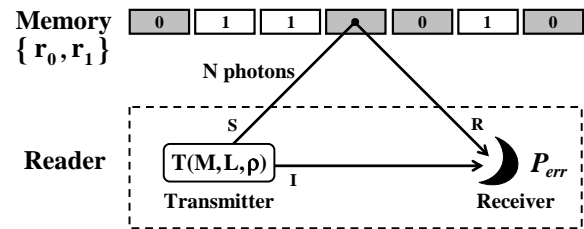


FIG. 1: **Model of classical memory.** Digital information is stored in a memory whose cells have different reflectivities:  $r = r_0$  encoding bit-value  $u = 0$ , and  $r = r_1$  encoding bit-value  $u = 1$ . **Readout of the memory.** In general, a digital reader consists of transmitter and receiver. The transmitter  $T(M, L, \rho)$  is a bipartite bosonic system, composed by a signal system  $S$  (with  $M$  modes) and an idler system  $I$  (with  $L$  modes), which is given in some global state  $\rho$ . The signal  $S$  emitted by this source has “bandwidth”  $M$  and “energy”  $N$  (total number of photons). The signal is directly shined over the cell, and its reflection  $R$  is detected together with the idler  $I$  at the output receiver, where a suitable measurement retrieves the value of the bit up to an error probability  $P_{err}$ .

Let us consider a digital memory where each cell can have two possible reflectivities,  $r_0$  or  $r_1$ , encoding the two values of a logical bit  $u$  (see Fig. 1). Close to the memory, we have a digital reader, made up of transmitter and receiver, whose goal is retrieving the value of the bit stored in a target cell. In general, we call “transmitter” a bipartite bosonic system, composed by a signal

system  $S$  with  $M$  modes and an idler system  $I$  with  $L$  modes, and globally given in some state  $\rho$ . This source can be completely specified by the notation  $T(M, L, \rho)$ . By definition, we say that the transmitter  $T$  is “classical” (“non-classical”) when the corresponding state  $\rho$  is classical (non-classical), i.e.,  $T_c = T(M, L, \rho_c)$  and  $T_{nc} = T(M, L, \rho_{nc})$  [12]. The signal  $S$  emitted by the transmitter is associated with two basic parameters: the total number of modes  $M$ , that we call “bandwidth” of the signal, and the total number of photons  $N$ , i.e., its “energy”. The signal  $S$  is directly shined on the target cell, and its reflection  $R$  is detected together with the idler  $I$  at the output receiver. Here a suitable measurement outputs the value of the bit up to an error probability  $P_{err}$ . Repeating the process for each cell of the memory, the reader retrieves an average of  $1 - H(P_{err})$  bits per cell, where  $H(\cdot)$  is the binary Shannon entropy.

The basic mechanism in our model of digital readout is the quantum channel discrimination. In fact, encoding a logical bit  $u \in \{0, 1\}$  in a pair of reflectivities  $\{r_0, r_1\}$  is equivalent to encoding  $u$  in a pair of attenuator channels  $\{\mathcal{E}(r_0), \mathcal{E}(r_1)\}$ , with linear losses  $\{r_0, r_1\}$  and acting on the signal modes. The readout of the bit consists in the statistical discrimination between  $r_0$  and  $r_1$ , which is formally equivalent to the channel discrimination between  $\mathcal{E}(r_0)$  and  $\mathcal{E}(r_1)$ . The error probability affecting the discrimination  $\mathcal{E}(r_0) \neq \mathcal{E}(r_1)$  depends on both transmitter and receiver. For a *fixed* transmitter  $T(M, L, \rho)$ , the pair  $\{\mathcal{E}(r_0), \mathcal{E}(r_1)\}$  generates two possible output states at the receiver,  $\sigma_0(T)$  and  $\sigma_1(T)$ . These are expressed by  $\sigma_u(T) = [\mathcal{E}(r_u)^{\otimes M} \otimes \mathcal{I}^{\otimes L}](\rho)$ , where  $\mathcal{E}(r_u)$  acts on the signals and the identity  $\mathcal{I}$  on the idlers. By optimizing over the output measurements, the minimum error probability which is achievable by the transmitter  $T$  in the channel discrimination  $\mathcal{E}(r_0) \neq \mathcal{E}(r_1)$  is equal to  $P_{err}(T) = (1 - D)/2$ , where  $D$  is the trace distance between  $\sigma_0(T)$  and  $\sigma_1(T)$ . Now the crucial point is the minimization of  $P_{err}(T)$  over the transmitters  $T$ . Clearly, this optimization must be constrained, by fixing the basic parameters of the signal. Here we consider the most general situation where only the signal energy  $N$  is fixed. Under this energy constraint, it is unknown the optimal transmitter  $T$  which minimizes  $P_{err}(T)$ . For this reason, it is non-trivial to ask the following question: does it exist a non-classical transmitter which outperforms any classical one? In other words: given two reflectivities  $\{r_0, r_1\}$ , i.e., two attenuator channels  $\{\mathcal{E}(r_0), \mathcal{E}(r_1)\}$ , and a fixed value  $N$  of the signal energy, can we find any  $T_{nc}$  such that  $P_{err}(T_{nc}) < P_{err}(T_c)$  for every  $T_c$ ? In the following we reply to this basic question, individuating remarkable physical regimes where the answer is positive. The first step in our derivation is providing a bound which is valid for every classical transmitter (see Appendix for the proof).

**Theorem 1 (classical discrimination bound)** *Let us consider the discrimination of two reflectivities  $\{r_0, r_1\}$  using a classical transmitter  $T_c$  which signals  $N$*

*photons. The corresponding error probability satisfies*

$$P_{err}(T_c) \geq \mathcal{C}(N, r_0, r_1) := \frac{1 - \sqrt{1 - e^{-N(\sqrt{r_1} - \sqrt{r_0})^2}}}{2}. \quad (1)$$

According to this theorem, all the classical transmitters  $T_c$  irradiating  $N$  photons on a memory with reflectivities  $\{r_0, r_1\}$  cannot beat the classical discrimination bound  $\mathcal{C}(N, r_0, r_1)$ , i.e., they cannot retrieve more than  $1 - H(\mathcal{C})$  bits per cell. Clearly, the next step is constructing a non-classical transmitter which can violate this bound. A possible design is the “EPR transmitter”, composed by  $M$  signals and  $M$  idlers, that are entangled pairwise via two-mode squeezing. This transmitter has the form  $T_{epr} = T(M, M, |\xi\rangle\langle\xi|^{\otimes M})$ , where  $|\xi\rangle\langle\xi|$  is a TMSV state entangling signal mode  $s \in S$  with idler mode  $i \in I$ . In the number-ket representation  $|\xi\rangle = (\cosh \xi)^{-1} \sum_{n=0}^{\infty} (\tanh \xi)^n |n\rangle_s |n\rangle_i$ , where the squeezing parameter  $\xi$  quantifies the signal-idler entanglement. An arbitrary EPR transmitter, composed by  $M$  copies of  $|\xi\rangle\langle\xi|$ , irradiates a signal with bandwidth  $M$  and energy  $N = M \sinh^2 \xi$ . As a consequence, this transmitter can be completely characterized by the basic parameters of the emitted signal, i.e., we can set  $T_{epr} = T_{M,N}$ . Then, let us consider the discrimination of two reflectivities  $\{r_0, r_1\}$  using an EPR transmitter  $T_{M,N}$  which signals  $N$  photons. The corresponding error probability can be upper-bounded via the quantum Chernoff bound [13, 14]

$$P_{err}(T_{M,N}) \leq \mathcal{Q}(M, N, r_0, r_1) := \frac{1}{2} \left[ \inf_{t \in (0,1)} \text{Tr}(\theta_0^t \theta_1^{1-t}) \right]^M, \quad (2)$$

where  $\theta_u := [\mathcal{E}(r_u) \otimes \mathcal{I}](|\xi\rangle\langle\xi|)$ . In other words, at least  $1 - H(\mathcal{Q})$  bits per cell can be retrieved from the memory. Exploiting Eqs. (1) and (2), our main question simplifies to finding  $\bar{M}$  such that  $\mathcal{Q}(\bar{M}, N, r_0, r_1) < \mathcal{C}(N, r_0, r_1)$ . In fact, this implies  $P_{err}(T_{\bar{M},N}) < \mathcal{C}(N, r_0, r_1)$ , i.e., the existence of an EPR transmitter  $T_{\bar{M},N}$  able to outperform any classical transmitter  $T_c$ . This is the result of the following theorem (see Appendix for the proof).

**Theorem 2 (threshold energy)** *For every pair of reflectivities  $\{r_0, r_1\}$  with  $r_0 \neq r_1$ , and signal energy*

$$N > N_{th}(r_0, r_1) := \frac{2 \ln 2}{2 - r_0 - r_1 - 2\sqrt{(1-r_0)(1-r_1)}}, \quad (3)$$

*there is a  $\bar{M}$  such that  $P_{err}(T_{\bar{M},N}) < \mathcal{C}(N, r_0, r_1)$ .*

Thus we get the central result of the paper: for every memory and above a threshold energy, there is an EPR transmitter which outperforms any classical transmitter. Remarkably, the threshold energy  $N_{th}$  turns out to be low ( $< 10^2$ ) for most of the memories  $\{r_0, r_1\}$  outside the region  $r_0 \approx r_1$ . This means that we can have an enhancement in the regime of few photons ( $N < 10^2$ ). Furthermore, for low energy  $N$ , the critical bandwidth  $\bar{M}$  can

be low too. In other words, in the regime of few photons, narrowband EPR transmitters are generally sufficient to overcome every classical transmitter. To confirm and quantify this analysis, we introduce the “minimum information gain”  $G(M, N, r_0, r_1) := 1 - H(\mathcal{Q}) - [1 - H(\mathcal{C})]$ . For given memory  $\{r_0, r_1\}$  and signal-energy  $N$ , this quantity lowerbounds the number of bits per cell which are gained by an EPR transmitter  $T_{M,N}$  over any classical transmitter  $T_c$  [15]. Numerical investigations (see Fig. 2) show that narrowband EPR transmitters are able to give  $G > 0$  in the regime of few photons and high reflectivities, corresponding to having  $r_0$  or  $r_1$  sufficiently close to 1 (as typical of optical disks). In this regime, part of the memories display remarkable gains ( $G > 0.5$ ).

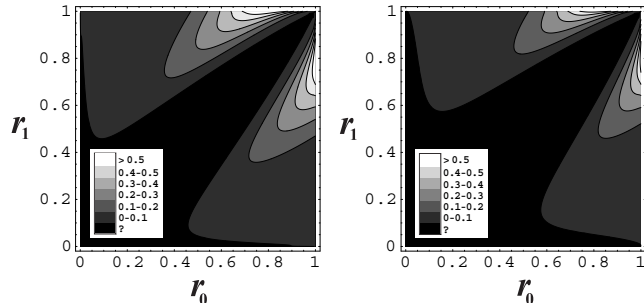


FIG. 2: **Left.** Minimum information gain  $G$  over the memory plane  $\{r_0, r_1\}$ . For a few-photon signal ( $N = 30$ ), we compare a narrowband EPR transmitter ( $M = 30$ ) with all the classical transmitters. Inside the black region ( $r_0 \approx r_1$ ) our investigation is inconclusive. Outside the black region, we have  $G > 0$ . **Right.**  $G$  plotted over the plane  $\{r_0, r_1\}$  in the presence of decoherence ( $\varepsilon = \bar{n} = 10^{-5}$ ). For a few-photon signal ( $N = 30$ ), we compare a narrowband EPR transmitter ( $M = 30$ ) with all the classical transmitters  $T(M, L, \rho_c)$  having  $M \leq M^* = 5 \times 10^6$ .

Thus the enhancement provided by quantum light can be dramatic in the regime of few photons and high reflectivities [16]. In order to investigate this regime more closely, we consider the case of ideal memories, defined by  $r_0 < r_1 = 1$ . As analytical result, we have the following theorem (see Appendix for the proof).

**Theorem 3 (ideal memory)** *For every  $r_0 < r_1 = 1$  and  $N \geq N_{th} := 1/2$ , there is a minimum bandwidth  $\bar{M}$  such that  $P_{err}(T_{M,N}) < \mathcal{C}(N, r_0, r_1)$  for every  $M > \bar{M}$ .*

Thus, for ideal memories and signals above  $N_{th} = 1/2$  photon, there are infinite EPR transmitters able to outperform every classical transmitter. For these memories, the threshold energy is so low that the regime of few photons can be fully explored. The gain  $G$  increases with the bandwidth, so that optimal performances are reached by broadband EPR transmitters ( $M \rightarrow \infty$ ). However, narrowband EPR transmitters are sufficient to give remarkable advantages, even for  $M = 1$  (i.e., using a single TMSV state). This is shown in Fig. 3, where  $G$  is plotted in terms of  $r_0$  and  $N$ , considering the two extreme cases  $M = 1$  and  $M \rightarrow \infty$ . According to Fig. 3, the value

of  $G$  can approach 1 for ideal memories and few photons even if we consider narrowband EPR transmitters.

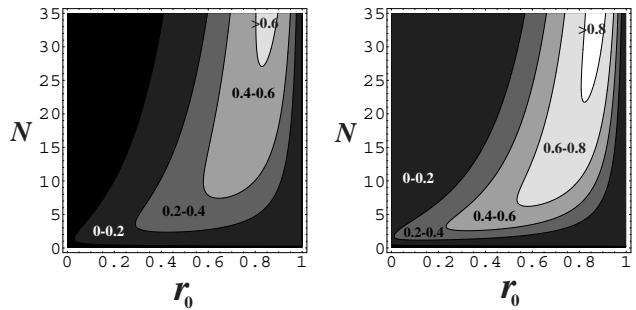


FIG. 3: Minimum information gain  $G$  versus  $r_0$  and  $N$ . Left picture refers to  $M = 1$ , right picture to  $M \rightarrow \infty$ . (For arbitrary  $M$  the scenario is intermediate.) Outside the inconclusive black region we have  $G > 0$ . For  $M \rightarrow \infty$  the black region is completely collapsed below  $N_{th} = 1/2$ .

*Presence of decoherence.* Note that the previous analysis does not consider the presence of thermal noise. Actually this is a good approximation in the optical range, where the number of thermal background photons is around  $10^{-26}$  at about  $1 \mu\text{m}$  and 300 K. However, to complete the analysis, we now show that the quantum effect exists even in the presence of stray photons hitting the upper side of the memory and decoherence within the reader. The scattering is modelled as white thermal noise with  $\bar{n}$  photons per mode entering each memory cell. Numerically we consider  $\bar{n} = 10^{-5}$  corresponding to non-trivial diffusion. This scenario may occur when the light, transmitted through the cells, is not readily absorbed by the drive (e.g., using a bucket detector just above the memory) but travels for a while diffusing photons which can hit the next cells. Assuming the presence of one photon per mode travelling the “optimistic distance” of one meter and undergoing Rayleigh scattering, we get roughly  $\bar{n} \simeq 10^{-5}$  [17]. The internal decoherence is modelled as a thermal channel  $\mathcal{N}(\varepsilon)$  adding Gaussian noise of variance  $\varepsilon$  to each signal/reflected mode, and  $2\varepsilon$  to the each idler mode (numerically we consider the non-trivial value  $\varepsilon = \bar{n} = 10^{-5}$ ). Now, distinguishing between two reflectivities  $\{r_0, r_1\}$  corresponds to discriminating between two Gaussian channels  $\mathcal{S}_u \otimes \mathcal{N}(2\varepsilon)$  for  $u \in \{0, 1\}$ . Here  $\mathcal{S}_u := \mathcal{N}(\varepsilon) \circ \mathcal{E}(r_u, \bar{n}) \circ \mathcal{N}(\varepsilon)$  acts on each signal mode, and contains the attenuator channel  $\mathcal{E}(r_u, \bar{n})$  with conditional loss  $r_u$  and thermal noise  $\bar{n}$ . To solve this problem we can use Theorem 1 with the proviso of generalizing the classical discrimination bound. In general, we have  $\mathcal{C} = (1 - \sqrt{1 - F^M})/2$ , where  $F$  is the fidelity between  $\mathcal{S}_0(|\sqrt{n_S}\rangle\langle\sqrt{n_S}|)$  and  $\mathcal{S}_1(|\sqrt{n_S}\rangle\langle\sqrt{n_S}|)$ , the two outputs of a single-mode coherent state  $|\sqrt{n_S}\rangle$  with  $n_S := N/M$  mean photons. Here the expression of  $\mathcal{C}$  depends also on the bandwidth  $M$  of the classical transmitter  $T_c = T(M, L, \rho_c)$ . Since  $\mathcal{C}$  decreases to zero for  $M \rightarrow +\infty$ , our quantum-classical comparison is now restricted to classical transmitters  $T(M, L, \rho_c)$  with  $M$  less than a maximal value  $M^* < +\infty$ . Remarkably we

find that, in the regime of few photons and high reflectivities, narrowband EPR transmitters are able to outperform all the classical transmitters up to an extremely large bandwidth  $M^*$ . This is confirmed by the numerical results of Fig. 2, proving the robustness of the quantum effect  $G > 0$  in the presence of decoherence. Notice that we can neglect classical transmitters with extremely large bandwidths (i.e., with  $M > M^*$ ) since they are not meaningful for the model. In fact, in a practical setting, the signal is an optical pulse with carrier frequency  $\omega$  high enough to completely resolve the target cell. This pulse has frequency bandwidth  $W \ll \omega$  and duration  $\tau \simeq W^{-1}$ . Assuming an output detector with response time  $\delta T \lesssim \tau$  and “reading time”  $T > \tau$ , the number of temporal modes which are excited is roughly  $M = WT$  [18, 19]. In other words, the bandwidth of the signal  $M$  is the product of its frequency bandwidth  $W$  and the reading time of the detector  $T$ . Now, the limit  $M \rightarrow +\infty$  corresponds to  $\delta T \rightarrow 0$  (infinite detector resolution) or  $T \rightarrow +\infty$  (infinite reading time). As a result, transmitters with too large  $M$  can be discarded.

*Sub-optimal receiver.* The former results are valid assuming an optimal output detection. Here we show an explicit receiver design which is (i) easy to construct experimentally and (ii) able to approximate the optimal results. This sub-optimal receiver consists of a continuous variable Bell measurement (i.e., a balanced beam-splitter followed by two homodyne detectors) whose output is classically processed by a suitable  $\chi^2$ -test with significance level  $\varphi$  (see Appendix for details). In this case the information gain  $G$  can be optimized jointly over the signal bandwidth  $M$  (i.e., the number of input TMSV states) and the significance level of the output test  $\varphi$ . As shown in Fig. 4, the superiority of quantum reading is fully preserved both in the absence and presence of decoherence.

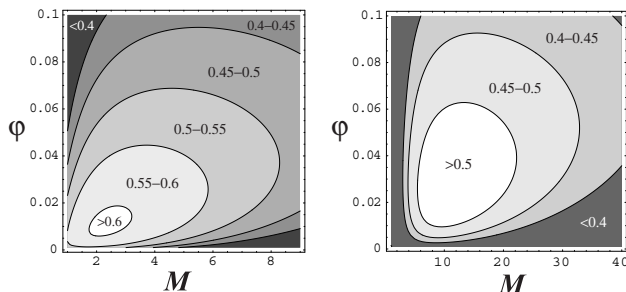


FIG. 4: **Left.** Information gain  $G$  optimized over the bandwidth  $M$  (i.e., number of TMSV states) and the significance level of the test  $\varphi$ . Note that  $G$  can be higher than 0.6 bits per cell. Results are shown in the absence of decoherence ( $\varepsilon = \bar{n} = 0$ ) considering  $r_0 = 0.85$ ,  $r_1 = 1$  and  $N = 35$ . **Right.**  $G$  optimized over  $M$  and  $\varphi$ . Results are shown in the presence of decoherence ( $\bar{n} = \varepsilon = 10^{-5}$ ) considering  $r_0 = 0.85$ ,  $r_1 = 0.95$ ,  $N = 100$  and  $M^* = 10^6$ .

*Discussion and conclusion.* The remarkable advantages of quantum reading are related with the regime of few photons, roughly given by  $N \simeq 1 \div 10^2$  photons per bit.

Note that this is very far from the energy which is used in today’s classical readers, roughly given by  $N \simeq 10^{10}$  photons per bit [20, 21].

In order to fully understand the advantages connected with the few-photon regime, let us fix the mean signal power  $P_S$  which is irradiated over the cell during the reading time. This quantity is approximately  $P_S = \hbar\omega NT^{-1}$ . Here, for fixed power  $P_S$ , we can decrease  $N$  together with  $T$ . In other words, the regime of few photons can be identified with the regime of short reading times, i.e., high data-transfer rates. Thus our results indicate the existence of quantum transmitters which allow reliable *ultra-fast* readout of digital memories. Besides this result, we have analogous consequences for the capacity. In fact, for fixed  $P_S$ , we can decrease  $N$  while increasing  $\omega$ . In other words, the regime of few photons can also be identified with the regime of high frequencies, i.e., high densities [22]. Thus we have also proven the existence of quantum transmitters which can read, reliably, *ultra-dense* digital memories.

The previous physical discussion (done for fixed signal power  $P_S$ ) can be generalized to include the “price to pay” for generating the light source. Given a global initial power  $P$ , we can write  $P_S = \kappa P$ , where the conversion factor  $\kappa$  depends on the source to be generated: typically  $\kappa \simeq 1$  for classical light, while  $\kappa \ll 1$  for non-classical light. Then, for fixed  $P$ , we have reading times  $T = O(\phi)$  and frequencies  $\omega = O(\phi^{-1})$ , where  $\phi := N/\kappa$ . Here the ratio  $\phi$  can still become extremely advantageous for quantum reading thanks to its superiority in the few-photon regime. For instance, today’s CDs are classically read using  $N \simeq 10^{10}$  photons per bit, so that  $\phi_{class} \simeq 10^{10}$  [20, 21]. Using spontaneous parametric down conversion in periodically poled KTP waveguides [23] we can generate EPR correlations around 810 nm with  $\kappa \simeq 10^{-9}$ . Exploiting this quantum source in the few-photon regime, e.g., using  $N \simeq 1$ , we can get  $\phi_{quant} \simeq 10^9$ , thus realizing shorter reading times already with current technology. Clearly this improvement will become dramatic as technology provides cheaper ways to create non-classical light (see, e.g., the recent achievements of Ref. [24]).

Besides these potentialities, there is another advantage provided by quantum light in the few-photon regime: the non-destructive readout of dye-based optical disks [21, 25]. For instance, if we try to increase the capacity of these devices using frequencies above the visible range, the organic layers may undergo a rapid UV-degradation [21, 26]. In this scenario, faint quantum light can retrieve the data safely, whereas classical light can only be destructive. From this perspective, our work shows new possible directions in the technology of organic memories.

*Acknowledgments.* S.P. was supported by a Marie Curie Action of the European Community. S.P. thanks S. L. Braunstein, A. Aspuru-Guzik, S. Lloyd, J. H. Shapiro, R. Nair, R. Munoz-Tapia, C. Ottaviani, N. Datta, M. Mosheni, J. Oppenheim, and C. Weedbrook for helpful discussions.

# Appendix

In this appendix, we start by providing some introductory notions on bosonic systems and Gaussian channels (see following Sec. I). Then, we explicitly connect our memory model with the basic problem of quantum channel discrimination (see following Sec. II). This connection is explicitly shown in two paradigmatic cases: the basic “pure-loss model”, where the memory cell is represented by a conditional-loss beam-splitter subject to vacuum noise, and the more general “thermal-loss model”, where thermal noise is added in order to include non-trivial effects of decoherence. In the subsequent sections we consider both these models and we provide the basic tools for making the quantum-classical comparison. In particular, in Sec. III, we provide the fundamental bound for studying classical transmitters, i.e., the “classical discrimination bound”. Then, in the next Sec. IV, we review the mathematical tools for studying EPR transmitters. By using these elements, we compare EPR and classical transmitters in Sec. V, where we explain in detail how to achieve the main results presented in our Letter. In particular, for the pure-loss model, we can provide analytical results: the “threshold energy” and “ideal memory” theorems, which are proven in Sec. VI. Finally, in Sec. VII, we show how the advantages of quantum reading persist when the optimal output detection is replaced by an easy-to-implement sub-optimal receiver, consisting of a continuous variable Bell measurement followed by a simple classical processing.

## I. BOSONIC SYSTEMS IN A NUTSHELL

A bosonic system with  $n$  modes is a quantum system described by a tensor-product Hilbert space  $\mathcal{H}^{\otimes n}$  and a vector of quadrature operators

$$\hat{\mathbf{x}}^T := (\hat{q}_1, \hat{p}_1, \dots, \hat{q}_n, \hat{p}_n), \quad (4)$$

satisfying the commutation relations [27]

$$[\hat{\mathbf{x}}, \hat{\mathbf{x}}^T] = 2i\mathbf{\Omega}, \quad (5)$$

where  $\mathbf{\Omega}$  is a symplectic form in  $\mathbb{R}^{2n}$ , i.e.,

$$\mathbf{\Omega} := \bigoplus_{i=1}^n \begin{pmatrix} 0 & 1 \\ -1 & 0 \end{pmatrix}. \quad (6)$$

By definition a quantum state  $\rho$  of a bosonic system is called “Gaussian” when its Wigner phase-space representation is Gaussian [28–30]. In such a case, the state is completely described by the first and second statistical moments. In other words, a Gaussian state  $\rho$  of  $n$  bosonic modes is characterized by a displacement vector

$$\bar{\mathbf{x}} := \text{Tr}(\hat{\mathbf{x}}\rho), \quad (7)$$

and a correlation matrix (CM)

$$\mathbf{V} := \frac{1}{2} \text{Tr} \left( \left\{ \hat{\mathbf{x}}, \hat{\mathbf{x}}^T \right\} \rho \right) - \bar{\mathbf{x}}\bar{\mathbf{x}}^T, \quad (8)$$

where  $\{, \}$  denotes the anticommutator [27]. The CM is a  $2n \times 2n$  real and symmetric matrix which must satisfy the uncertainty principle [31, 32]

$$\mathbf{V} + i\mathbf{\Omega} \geq 0. \quad (9)$$

An important example of Gaussian state is the TMSV state for two bosonic modes  $\{s, i\}$  (whose number-ket representation is given in the Letter). This state has zero mean ( $\bar{\mathbf{x}} = 0$ ) and its CM is given by

$$\mathbf{V} = \begin{pmatrix} (2n_S + 1)\mathbf{I} & 2\sqrt{n_S(n_S + 1)}\mathbf{Z} \\ 2\sqrt{n_S(n_S + 1)}\mathbf{Z} & (2n_S + 1)\mathbf{I} \end{pmatrix}, \quad (10)$$

where  $n_S \geq 0$  and

$$\mathbf{I} = \begin{pmatrix} 1 & 0 \\ 0 & 1 \end{pmatrix}, \quad \mathbf{Z} = \begin{pmatrix} 1 & 0 \\ 0 & -1 \end{pmatrix}. \quad (11)$$

Here  $n_S$  represents the mean number of thermal photons which are present in each mode. This number is connected with the “two-mode squeezing parameter” [33] by the relation

$$n_S = \sinh^2 \xi. \quad (12)$$

Parameter  $\xi$  completely characterizes the state (therefore denoted by  $|\xi\rangle \langle \xi|$ ) and quantifies the entanglement between the two modes  $s$  and  $i$  (being an entanglement monotone for this class of states).

Another important example of Gaussian state is the (multimode) coherent state. For  $K$  modes this is given by

$$|\boldsymbol{\alpha}\rangle \langle \boldsymbol{\alpha}| = \bigotimes_{i=1}^K |\alpha_i\rangle \langle \alpha_i|, \quad (13)$$

where  $\boldsymbol{\alpha} := (\alpha_1, \dots, \alpha_K)$  is a row-vector of amplitudes  $\alpha_i = (q_i + ip_i)/2$ . This state has CM equal to the identity and, therefore, is completely characterized by its displacement vector  $\bar{\mathbf{x}}$ , which is determined by  $\boldsymbol{\alpha}$ . Starting from the coherent states, we can characterize all the possible states of a bosonic system by introducing the P-representation. In fact, a generic state  $\rho$  of  $K$  bosonic modes can be decomposed as

$$\rho = \int d^{2K} \boldsymbol{\alpha} \mathcal{P}(\boldsymbol{\alpha}) |\boldsymbol{\alpha}\rangle \langle \boldsymbol{\alpha}|, \quad (14)$$

where  $\mathcal{P}(\boldsymbol{\alpha})$  is a quasi-probability distribution, i.e., normalized to 1 but generally non-positive (here we use the compact notation  $\int d^{2K} \boldsymbol{\alpha} := \int d^2 \alpha_1 \dots \int d^2 \alpha_K$ ). By definition, a bosonic state  $\rho$  is called “classical” if  $\mathcal{P}(\boldsymbol{\alpha})$  is positive, i.e.,  $\mathcal{P}$  is a proper probability distribution. By contrast, the state is called “non-classical” when  $\mathcal{P}(\boldsymbol{\alpha})$  is non-positive. It is clear that a classical state is separable, since Eq. (14) with  $\mathcal{P}$  positive corresponds to a state preparation via local operations and classical communications (LOCCs). The borderline between classical and non-classical states is given by the coherent states, for

which  $\mathcal{P}$  is a delta function. Note also that the classical states are generally non-Gaussian. In fact, one can have a classical state given by a *finite ensemble* of coherent states (whose  $\mathcal{P}$ -representation corresponds to a sum of Dirac-deltas).

In general we use the formalism  $T(M, L, \rho)$  to denote a “bipartite transmitter” or, more simply, a “transmitter”. This is a compact notation for characterizing simultaneously a bipartite bosonic system and its state. More specifically,  $M$  and  $L$ , represent the number of modes present in two partitions of the system, called signal (sub)system  $S$  and idler (sub)system  $I$ . Then, given this bipartite system,  $\rho$  represents the corresponding global state. This notation is very useful when both system and state are variable. By definition, a “transmitter”  $T(M, L, \rho)$  is classical (non-classical) when its state  $\rho$  is classical (non-classical), i.e.,  $T_c = T(M, L, \rho_c)$  and  $T_{nc} = T(M, L, \rho_{nc})$ . In the comparison between different transmitters, one has to fix some of the parameters of the signal (sub)system  $S$ . The basic parameters of  $S$  are the total number of signal modes  $M$  (signal bandwidth) and the total number of signal photons  $N$  (signal energy).

### A. Gaussian channels

A Gaussian channel is a completely positive trace-preserving (CPTP) map

$$\mathcal{E} : \rho \rightarrow \sigma := \mathcal{E}(\rho) \quad (15)$$

which transforms Gaussian states into Gaussian states. In particular, a one-mode Gaussian channel (i.e., acting on one-mode bosonic states) can be easily described in terms of the statistical moments  $\{\bar{\mathbf{x}}, \mathbf{V}\}$ . This channel corresponds to the transformation [34–36]

$$\mathbf{V} \rightarrow \mathbf{K}\mathbf{V}\mathbf{K}^T + \mathbf{N}, \quad \bar{\mathbf{x}} \rightarrow \mathbf{K}\bar{\mathbf{x}} + \mathbf{d}, \quad (16)$$

where  $\mathbf{d}$  is an  $\mathbb{R}^2$ -vector, while  $\mathbf{K}$  and  $\mathbf{N}$  are  $2 \times 2$  real matrices, with  $\mathbf{N}^T = \mathbf{N} \geq 0$  and

$$\det \mathbf{N} \geq (\det \mathbf{K} - 1)^2. \quad (17)$$

Important examples of one-mode Gaussian channels are the following:

- (i) The “attenuator channel”  $\mathcal{E}(r, \bar{n})$  with loss  $r \in [0, 1]$  and thermal noise  $\bar{n} \geq 0$ . This channel can be represented by a beam splitter with reflectivity  $r$  which mixes the input mode with a bath mode prepared in a thermal state with  $\bar{n}$  mean photons. This channel implements the transformation of Eq. (16) with

$$\mathbf{K} = \sqrt{r}\mathbf{I}, \quad \mathbf{N} = (1 - r)(2\bar{n} + 1)\mathbf{I}, \quad (18)$$

and  $\mathbf{d} = 0$ . In particular, when the thermal noise  $\bar{n}$  is negligible, the attenuator channel  $\mathcal{E}(r) := \mathcal{E}(r, 0)$  is represented by a beam splitter with reflectivity  $r$  and a vacuum bath mode.

- (ii) The thermal channel  $\mathcal{N}(\varepsilon)$  adding Gaussian noise with variance  $\varepsilon \geq 0$ . This channel implements the transformation of Eq. (16) with

$$\mathbf{K} = \mathbf{I}, \quad \mathbf{N} = \varepsilon\mathbf{I}, \quad (19)$$

and  $\mathbf{d} = 0$ . This kind of channel is suitable to describe the effects of decoherence when the loss is negligible. This is a typical situation within optical apparatuses which are small in size (as is the case of our memory reader).

It is clear that, for every pair of Gaussian channels,  $\mathcal{E}$  and  $\mathcal{E}'$ , acting on the same state space, their composition  $\mathcal{E} \circ \mathcal{E}'$  is also Gaussian channel. If  $\mathcal{E}$  and  $\mathcal{E}'$  are Gaussian channels acting on two different spaces, their tensor product  $\mathcal{E} \otimes \mathcal{E}'$  is also Gaussian. Hereafter we call “bipartite Gaussian channel” a Gaussian channel which is in the tensor-product form  $\mathcal{E} \otimes \mathcal{E}'$ . The action of a bipartite Gaussian channel on a two-mode bosonic state is very simple in terms of its second statistical moments. In fact, let us consider two bosonic modes,  $A$  and  $B$ , in a state  $\rho_{AB}$  with generic CM

$$\mathbf{V} = \begin{pmatrix} \mathbf{A} & \mathbf{C} \\ \mathbf{C}^T & \mathbf{B} \end{pmatrix}, \quad (20)$$

where  $\mathbf{A}$ ,  $\mathbf{B}$  and  $\mathbf{C}$  are  $2 \times 2$  real matrices. At the output of a bipartite Gaussian channel  $\mathcal{E}^{A \otimes B} := \mathcal{E}_A \otimes \mathcal{E}_B$ , we have the CM

$$\mathbf{V}_{out} = \begin{pmatrix} \mathbf{K}_A \mathbf{A} \mathbf{K}_A^T + \mathbf{N}_A & \mathbf{K}_A \mathbf{C} \mathbf{K}_B^T \\ \mathbf{K}_B \mathbf{C}^T \mathbf{K}_A^T & \mathbf{K}_B \mathbf{B} \mathbf{K}_B^T + \mathbf{N}_B \end{pmatrix}, \quad (21)$$

where the matrices  $(\mathbf{K}_A, \mathbf{N}_A)$  refer to  $\mathcal{E}_A$  (acting on the first mode), while  $(\mathbf{K}_B, \mathbf{N}_B)$  refer to  $\mathcal{E}_B$  (acting on the second mode).

**Proof.** Both the channels  $\mathcal{E}_A \otimes \mathcal{E}_B$  are dilated, so that we have

$$\mathcal{E}^{A \otimes B}(\rho_{AB}) = \text{Tr}_{A'B'} [(U_{A'A} \otimes U_{BB'}) \times (|0\rangle\langle 0|_{A'} \otimes \rho_{AB} \otimes |0\rangle\langle 0|_{B'}) (U_{A'A}^\dagger \otimes U_{BB'}^\dagger)], \quad (22)$$

where  $A'$  and  $B'$  are supplementary sets of bosonic modes prepared in vacua, while  $U_{A'A}$  and  $U_{BB'}$  are Gaussian unitaries. According to Eq. (22), the input CM  $\mathbf{V}$  is subject to three subsequent operations. First, it must be dilated to  $\mathbf{I}_{A'} \oplus \mathbf{V} \oplus \mathbf{I}_{B'}$ , where  $\mathbf{I}_{A'}$  and  $\mathbf{I}_{B'}$  are identity matrices of suitable dimensions. Then, it is transformed via congruence by  $\mathbf{S}_{A'A} \oplus \mathbf{S}_{B'B}$ , where  $\mathbf{S}_{A'A}$  and  $\mathbf{S}_{B'B}$  are the symplectic matrices corresponding to  $U_{A'A}$  and  $U_{BB'}$ , respectively. Finally, rows and columns corresponding to  $A'$  and  $B'$  are elided (trace). By setting

$$\mathbf{S}_{A'A} = \begin{pmatrix} \mathbf{a} & \mathbf{c} \\ \mathbf{d} & \mathbf{b} \end{pmatrix}, \quad \mathbf{S}_{B'B} = \begin{pmatrix} \mathbf{e} & \mathbf{g} \\ \mathbf{h} & \mathbf{f} \end{pmatrix}, \quad (23)$$

we get

$$\mathbf{V}_{out} = \begin{pmatrix} \mathbf{bAb}^T + \mathbf{d}\mathbf{d}^T & \mathbf{bCe}^T \\ \mathbf{eC}^T\mathbf{b}^T & \mathbf{eBe}^T + \mathbf{g}\mathbf{g}^T \end{pmatrix}. \quad (24)$$

Now, by setting

$$\mathbf{K}_A := \mathbf{b}, \mathbf{N}_A := \mathbf{d}\mathbf{d}^T, \quad (25)$$

and

$$\mathbf{K}_B := \mathbf{e}, \mathbf{N}_B := \mathbf{g}\mathbf{g}^T, \quad (26)$$

we get exactly Eq. (21). ■

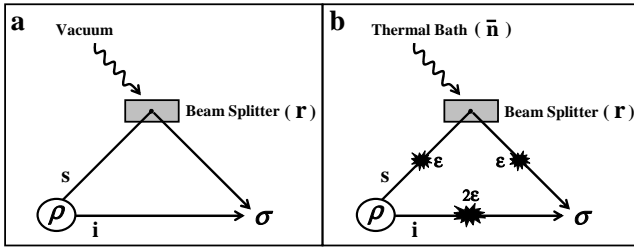


FIG. 5: **Inset a.** Pure-loss model, implementing the bipartite Gaussian channel  $\mathcal{G} = \mathcal{E} \otimes \mathcal{I}$ . **Inset b.** Thermal-loss model, implementing the bipartite Gaussian channel  $\mathcal{G} = \mathcal{S} \otimes \mathcal{D}$  (see text).

## II. MEMORY MODEL AND GAUSSIAN CHANNEL DISCRIMINATION

Let us consider the beam-splitter scheme of Fig. 5a, where an input state  $\rho$  of two modes (“signal mode”  $s$  and “idler mode”  $i$ ) is transformed into an output state  $\sigma$ . Hereafter we call this scheme the “pure-loss model”. The corresponding transformation is a bipartite Gaussian channel

$$\mathcal{G} = \mathcal{E}(r) \otimes \mathcal{I}, \quad (27)$$

where the attenuator channel  $\mathcal{E}(r)$  acts on the signal mode, and the identity channel  $\mathcal{I}$  acts on the idler mode. By construction,  $\mathcal{G}$  is a memoryless channel. Thus, if we consider a transmitter  $T(M, L, \rho)$ , i.e.,  $M$  signal modes  $s \in S$  and  $L$  idler modes  $i \in I$  in a multimode state  $\rho$ , the input state is transformed into the output state

$$\sigma = \mathcal{G}^{M,L}(\rho), \quad (28)$$

where

$$\mathcal{G}^{M,L} := \mathcal{E}(r)^{\otimes M} \otimes \mathcal{I}^{\otimes L}. \quad (29)$$

This is schematically depicted in Fig. 6.

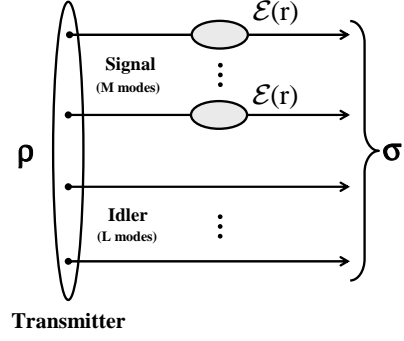


FIG. 6: Visual representation of Eq. (29).

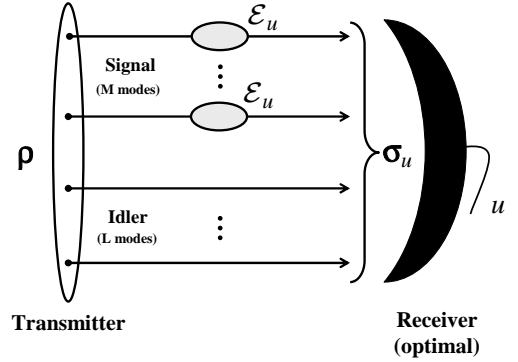


FIG. 7: Channel discrimination problem (pure-loss model).

Now, encoding a logical bit  $u = 0, 1$  in the reflectivity of the beam splitter  $r = r_u$  corresponds to encoding the bit into the conditional attenuator channel  $\mathcal{E}_u := \mathcal{E}(r_u)$ . Thus, reading a memory cell using an input transmitter  $T(M, L, \rho)$ , and an output receiver, corresponds to the channel discrimination problem depicted in Fig. 7. The error probability in the decoding of the logical bit, i.e.,

$$P_{err} = \frac{P(u = 0|u = 1) + P(u = 1|u = 0)}{2} \quad (30)$$

corresponds to the error probability of discriminating between the two equiprobable channels  $\mathcal{E}_0$  and  $\mathcal{E}_1$ . The minimization of this error probability involves the optimization of both input and output. For a *fixed* input  $T(M, L, \rho)$ , we have two equiprobable output states,  $\sigma_0$  and  $\sigma_1$ , with

$$\sigma_u = \mathcal{G}_u^{M,L}(\rho) = (\mathcal{E}_u^{\otimes M} \otimes \mathcal{I}^{\otimes L})(\rho). \quad (31)$$

The optimal measurement for their discrimination is given by the dichotomic POVM [18]

$$E_0 = \Pi(\gamma_+), \quad E_1 = I - \Pi(\gamma_+), \quad (32)$$

where  $\Pi(\gamma_+)$  is the projector onto the positive part  $\gamma_+$  of the Helstrom matrix  $\gamma := \sigma_0 - \sigma_1$  [38]. Using this measurement, the two output states,  $\sigma_0$  and  $\sigma_1$ , are discriminated with a *minimum* error probability which is

provided by the Helstrom bound, i.e.,

$$P_{err}(\sigma_0 \neq \sigma_1) = \frac{1 - D(\sigma_0, \sigma_1)}{2}, \quad (33)$$

where  $D(\sigma_0, \sigma_1)$  is the trace distance between  $\sigma_0$  and  $\sigma_1$  [18]. In particular,

$$D(\sigma_0, \sigma_1) := \frac{1}{2} \|\sigma_0 - \sigma_1\|_1, \quad (34)$$

where  $\|\gamma\|_1 := \text{Tr} \sqrt{\gamma^\dagger \gamma}$  is the trace norm. Thus, given two equiprobable channels  $\{\mathcal{E}_0, \mathcal{E}_1\}$  and a *fixed* input transmitter  $T$ , we can always assume an optimal output detection. Under this assumption (optimal detection), the channel discrimination problem  $\mathcal{E}_0 \neq \mathcal{E}_1$  with fixed transmitter  $T = T(M, L, \rho)$  is fully characterized by the conditional error probability

$$P_{err}(\mathcal{E}_0 \neq \mathcal{E}_1|T) := \left[ \frac{1 - D(\sigma_0, \sigma_1)}{2} \right]_{\sigma_u = (\mathcal{E}_u^{\otimes M} \otimes \mathcal{I}^{\otimes L})(\rho)}. \quad (35)$$

Now, the minimal error probability for discriminating  $\mathcal{E}_0$  and  $\mathcal{E}_1$  is given by optimizing the previous quantity over all the input transmitters, i.e.,

$$P_{err}(\mathcal{E}_0 \neq \mathcal{E}_1) = \min_T P_{err}(\mathcal{E}_0 \neq \mathcal{E}_1|T). \quad (36)$$

In general, this error probability tends to zero in the limit of infinite energy  $N \rightarrow +\infty$  (this happens whenever  $\mathcal{E}_0 \neq \mathcal{E}_1$ ). For this reason, in order to consider a non-trivial quantity, we must fix the signal-energy  $N$  in the previous minimization. Let us denote by  $T|N$  the class of transmitters signalling  $N$  photons. Then, we can define the conditional error probability

$$P_{err}(\mathcal{E}_0 \neq \mathcal{E}_1|N) = \min_{T|N} P_{err}(\mathcal{E}_0 \neq \mathcal{E}_1|T). \quad (37)$$

It is an *open question* to find the optimal transmitter within the class  $T|N$ , i.e., realizing the minimization of Eq. (37). The central idea of our Letter is a direct consequence of this open question. In fact, strictly connected with this question, there is another fundamental problem, whose resolution sensibly narrows the search for optimal transmitters: within the conditional class  $T|N$ , can we find a non-classical transmitter which outperforms any classical transmitter? More exactly, given two attenuator channels  $\{\mathcal{E}_0, \mathcal{E}_1\}$  and fixed signal-energy  $N$ , can we find any  $T_{nc}$  such that

$$P_{err}(\mathcal{E}_0 \neq \mathcal{E}_1|T_{nc}) < P_{err}(\mathcal{E}_0 \neq \mathcal{E}_1|T_c), \quad (38)$$

for every  $T_c$ ? In our Letter we solve this problem [37]. In particular, we show this is possible for an important physical regime, i.e., for channels  $\{\mathcal{E}_0, \mathcal{E}_1\}$  corresponding to high-reflectivities (as typical of optical memories) and signals with few photons (as typical of entanglement sources).

## A. Introducing thermal noise

In general, the pure-loss model of Fig. 5a represents a very good description in the optical range if we assume the use of a good reading apparatus. To complete the analysis and show the robustness of the model with respect to decoherence, we also consider the presence of thermal noise, as explicitly stated in the Letter. The noisy scenario is the one depicted in Fig. 5b, that we call the “thermal-loss model”. This corresponds to the bipartite Gaussian channel

$$\mathcal{G} = \mathcal{S} \otimes \mathcal{D}, \quad (39)$$

where

$$\mathcal{S} := \mathcal{N}(\varepsilon) \circ \mathcal{E}(r, \bar{n}) \circ \mathcal{N}(\varepsilon) = \mathcal{S}(r, \bar{n}, \varepsilon) \quad (40)$$

acts on the signal mode, and

$$\mathcal{D} = \mathcal{N}(\varepsilon) \circ \mathcal{N}(\varepsilon) = \mathcal{N}(2\varepsilon) \quad (41)$$

acts on the idler mode. Exactly as before,  $\mathcal{G}$  represents a memoryless channel. As a result, the state  $\rho$  of an input transmitter  $T(M, L, \rho)$  is transformed into an output state  $\sigma = \mathcal{G}^{M,L}(\rho)$ , where

$$\mathcal{G}^{M,L} := \mathcal{S}^{\otimes M} \otimes \mathcal{D}^{\otimes L}. \quad (42)$$

This transformation is depicted in Fig. 8. Now, encoding a logical bit  $u = 0, 1$  in the reflectivity of the beam splitter  $r = r_u$  corresponds to encoding the bit into the Gaussian channel  $\mathcal{S}_u := \mathcal{S}(r_u, \bar{n}, \varepsilon)$ . It follows that the readout of our memory cell corresponds to the channel discrimination problem depicted in Fig. 9.

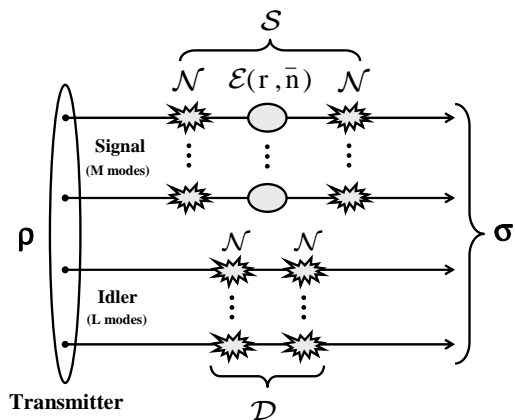


FIG. 8: Visual representation of Eq. (42).

It is clear that the present thermal scenario (Fig. 9) can be formally achieved by the previous non-thermal one (Fig. 7) via the replacements

$$\mathcal{E}_u \rightarrow \mathcal{S}_u, \quad \mathcal{I} \rightarrow \mathcal{D}. \quad (43)$$

In this case, the idlers are subject to a non-trivial decoherence channel  $\mathcal{D}$ , which plays an active role in the



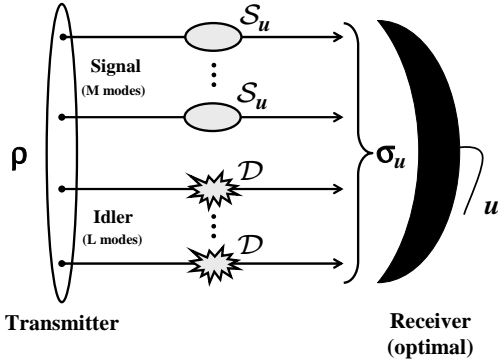


FIG. 9: Channel discrimination problem (thermal-loss model).

discrimination problem. In general, this problem can be formulated as the discrimination of two *bipartite* channels,  $\mathcal{G}_0 = \mathcal{S}_0 \otimes \mathcal{D}$  and  $\mathcal{G}_1 = \mathcal{S}_1 \otimes \mathcal{D}$ , using a transmitter  $T = T(M, L, \rho)$  and an optimal receiver. The corresponding error probability is defined by

$$P_{err}(\mathcal{G}_0 \neq \mathcal{G}_1|T) := \left[ \frac{1 - D(\sigma_0, \sigma_1)}{2} \right]_{\sigma_u = (\mathcal{S}_u^{\otimes M} \otimes \mathcal{D}^{\otimes L})(\rho)}. \quad (44)$$

Clearly this problem is more difficult to study. For this reason, our basic question becomes the following: given two bipartite channels  $\{\mathcal{G}_0, \mathcal{G}_1\}$  and fixed signal-energy  $N$ , can we find any  $T_{nc}$  such that

$$P_{err}(\mathcal{G}_0 \neq \mathcal{G}_1|T_{nc}) < P_{err}(\mathcal{G}_0 \neq \mathcal{G}_1|T_c), \quad (45)$$

for a *suitable large class* of  $T_c$ ? As stated in the Letter (and explicitly shown afterwards), we can give a positive answer to this question too. This is possible by excluding broadband classical transmitters which are not meaningful for the model (see the Letter for a physical discussion).

In the following Secs. III and IV we introduce the basic tools that we need to compare classical and non-classical transmitters, in both the models: pure-loss and thermal-loss. In particular, Sec. III provides one of the central results of the work: the ‘‘classical discrimination bound’’, which enables us to bound all the classical transmitters. Then, Sec. IV concerns the study of the non-classical EPR transmitter. At that point we have all the elements to make the comparison, i.e., replying to the questions in Eqs. (38) and (45). This comparison is thoroughly discussed in Sec. V. In particular, for the pure-loss model, we can also derive analytical results, as shown in Sec. VI. These results are the ‘‘threshold energy’’ theorem and the ‘‘ideal memory’’ theorem.

### III. CLASSICAL DISCRIMINATION BOUND

#### A. Thermal-loss model

Let us consider the discrimination of two bipartite Gaussian channels

$$\mathcal{G}_0 = \mathcal{S}_0 \otimes \mathcal{D} = \mathcal{G}(r_0, \bar{n}, \varepsilon), \quad (46)$$

and

$$\mathcal{G}_1 = \mathcal{S}_1 \otimes \mathcal{D} = \mathcal{G}(r_1, \bar{n}, \varepsilon), \quad (47)$$

by using a bipartite transmitter  $T = T(M, L, \rho)$  which signals  $N$  photons. The global input state can be decomposed using the following bipartite  $\mathcal{P}$ -representation [4, 39]

$$\rho = \int d^{2M} \alpha \int d^{2L} \beta \mathcal{P}(\alpha, \beta) |\alpha\rangle_S \langle \alpha| \otimes |\beta\rangle_I \langle \beta|, \quad (48)$$

where  $\alpha := (\alpha_1, \dots, \alpha_M)$  is a vector of amplitudes for the signal  $M$ -mode coherent-state

$$|\alpha\rangle_S \langle \alpha| = \bigotimes_{k=1}^M |\alpha_k\rangle \langle \alpha_k|, \quad (49)$$

and  $\beta := (\beta_1, \dots, \beta_L)$  is a vector of amplitudes for the idler  $L$ -mode coherent-state

$$|\beta\rangle_I \langle \beta| = \bigotimes_{k=1}^L |\beta_k\rangle \langle \beta_k|. \quad (50)$$

The reduced state for the  $M$  signal modes is given by

$$\rho_S = \int d^{2M} \alpha \mathcal{P}(\alpha) |\alpha\rangle_S \langle \alpha|, \quad (51)$$

where

$$\mathcal{P}(\alpha) := \int d^{2L} \beta \mathcal{P}(\alpha, \beta). \quad (52)$$

The total (mean) number of photons in the  $M$ -mode signal system can be written as

$$N = \int d^{2M} \alpha \mathcal{P}(\alpha) E, \quad (53)$$

where

$$E := \sum_{k=1}^M |\alpha_k|^2. \quad (54)$$

Now, conditioned on the value of the bit ( $u = 0$  or  $1$ ), the global output state at the receiver can be written as

$$\sigma_u = \int d^{2M} \alpha \int d^{2L} \beta \mathcal{P}(\alpha, \beta) \sigma_u(\alpha) \otimes \gamma(\beta), \quad (55)$$

where

$$\sigma_u(\boldsymbol{\alpha}) := \mathcal{S}_u^{\otimes M}(|\boldsymbol{\alpha}\rangle_S \langle \boldsymbol{\alpha}|) = \bigotimes_{k=1}^M \mathcal{S}_u(|\alpha_k\rangle \langle \alpha_k|), \quad (56)$$

and

$$\gamma(\boldsymbol{\beta}) := \mathcal{D}^{\otimes L}(|\boldsymbol{\beta}\rangle_I \langle \boldsymbol{\beta}|) = \bigotimes_{k=1}^L \mathcal{D}(|\beta_k\rangle \langle \beta_k|). \quad (57)$$

Assuming an optimal detection of all the output modes (signals and idlers), the error probability in the channel discrimination (i.e., bit decoding) is given by

$$P_{err}(\mathcal{G}_0 \neq \mathcal{G}_1|T) = \frac{1}{2} [1 - D(\sigma_0, \sigma_1)], \quad (58)$$

where  $\sigma_0$  and  $\sigma_1$  are specified by Eq. (55) for  $u = 0, 1$ .

The study of this error probability can be greatly simplified in the case of classical transmitters. In fact, by assuming a classical transmitter  $T_c = T(M, L, \rho_c)$ , the  $\mathcal{P}$ -representation of Eq. (48) is positive. As a consequence, the error probability can be lower-bounded by a quantity which depends on the signal parameters only, i.e.,

$$P_{err}(\mathcal{G}_0 \neq \mathcal{G}_1|T_c) \geq \mathcal{C}(M, N). \quad (59)$$

In other words, for fixed  $\mathcal{G}_0$  and  $\mathcal{G}_1$ , we can write a lower bound which holds for all the classical transmitters emitting signals with bandwidth  $M$  and energy  $N$ . This is the basic result stated in the following theorem.

**Theorem 4** *Let us consider the discrimination of two bipartite Gaussian channels,  $\mathcal{G}_0 = \mathcal{S}_0 \otimes \mathcal{D} = \mathcal{G}(r_0, \bar{n}, \varepsilon)$  and  $\mathcal{G}_1 = \mathcal{S}_1 \otimes \mathcal{D} = \mathcal{G}(r_1, \bar{n}, \varepsilon)$ , by using a classical transmitter  $T_c = T(M, L, \rho_c)$  which signals  $N$  photons. The corresponding error probability  $P_{err}(\mathcal{G}_0 \neq \mathcal{G}_1|T_c)$  is lower-bounded ( $\geq$ ) by*

$$\mathcal{C}(M, N) := \frac{1 - \sqrt{1 - F(n_S)^M}}{2}, \quad (60)$$

where  $F(n_S)$  is the fidelity between  $\mathcal{S}_0(|\sqrt{n_S}\rangle \langle \sqrt{n_S}|)$  and  $\mathcal{S}_1(|\sqrt{n_S}\rangle \langle \sqrt{n_S}|)$ , the two outputs of a single-mode coherent state  $|\sqrt{n_S}\rangle$  with  $n_S := N/M$  mean photons. In particular, in terms of all the parameters, we have

$$F(n_S) = \omega^{-1} \exp(-\lambda n_S), \quad (61)$$

where  $\omega$  and  $\lambda$  are defined by

$$\omega := \frac{1}{2} \left[ \xi_0 \xi_1 + 1 - \sqrt{(\xi_0^2 - 1)(\xi_1^2 - 1)} \right] \geq 1, \quad (62)$$

and

$$\lambda := \frac{2(\sqrt{r_0} - \sqrt{r_1})^2}{\xi_0 + \xi_1} \geq 0, \quad (63)$$

with

$$\xi_u := 1 + 2\bar{n}(1 - r_u) + \varepsilon(1 + r_u) \geq 1. \quad (64)$$

**Proof.** The two possible states,  $\sigma_0$  and  $\sigma_1$ , describing the whole set of output modes (signals and idlers) are given by Eq. (55), under the assumption that  $\mathcal{P}(\boldsymbol{\alpha}, \boldsymbol{\beta})$  is positive. In order to lowerbound the error probability

$$P_{err}(\mathcal{G}_0 \neq \mathcal{G}_1|T_c) = \frac{1}{2} [1 - D(\sigma_0, \sigma_1)], \quad (65)$$

we upperbound the trace distance  $D(\sigma_0, \sigma_1)$ . Since  $\mathcal{P}(\boldsymbol{\alpha}, \boldsymbol{\beta})$  is a proper probability distribution, we can use the joint convexity of the trace distance [1]. Using this property, together with the stability of the trace distance under addition of systems [1], we get

$$\begin{aligned} D(\sigma_0, \sigma_1) &\leq \int d^{2M} \boldsymbol{\alpha} \int d^{2L} \boldsymbol{\beta} \mathcal{P}(\boldsymbol{\alpha}, \boldsymbol{\beta}) \times \\ &D[\sigma_0(\boldsymbol{\alpha}) \otimes \gamma(\boldsymbol{\beta}), \sigma_1(\boldsymbol{\alpha}) \otimes \gamma(\boldsymbol{\beta})] = \\ &\int d^{2M} \boldsymbol{\alpha} \int d^{2L} \boldsymbol{\beta} \mathcal{P}(\boldsymbol{\alpha}, \boldsymbol{\beta}) D[\sigma_0(\boldsymbol{\alpha}), \sigma_1(\boldsymbol{\alpha})] = \\ &\int d^{2M} \boldsymbol{\alpha} \mathcal{P}(\boldsymbol{\alpha}) D[\sigma_0(\boldsymbol{\alpha}), \sigma_1(\boldsymbol{\alpha})], \end{aligned} \quad (66)$$

where  $\mathcal{P}(\boldsymbol{\alpha})$  is the marginal distribution defined in Eq. (52). In general, it is known that [40, 41]

$$D(\rho, \sigma) \leq \sqrt{1 - F(\rho, \sigma)}, \quad (67)$$

for every pair of quantum states  $\rho$  and  $\sigma$ . As a consequence, we can immediately write

$$D[\sigma_0(\boldsymbol{\alpha}), \sigma_1(\boldsymbol{\alpha})] \leq \sqrt{1 - F[\sigma_0(\boldsymbol{\alpha}), \sigma_1(\boldsymbol{\alpha})]}, \quad (68)$$

where  $F[\sigma_0(\boldsymbol{\alpha}), \sigma_1(\boldsymbol{\alpha})]$  is the fidelity between the two outputs  $\sigma_0(\boldsymbol{\alpha})$  and  $\sigma_1(\boldsymbol{\alpha})$  defined by Eq. (56). Now we can exploit the multiplicativity of the fidelity under tensor products of density operators. In other words, we can decompose

$$\begin{aligned} F[\sigma_0(\boldsymbol{\alpha}), \sigma_1(\boldsymbol{\alpha})] &= \\ F \left[ \bigotimes_{k=1}^M \mathcal{S}_0(|\alpha_k\rangle \langle \alpha_k|), \bigotimes_{k=1}^M \mathcal{S}_1(|\alpha_k\rangle \langle \alpha_k|) \right] &= \\ \prod_{k=1}^M F[\mathcal{S}_0(|\alpha_k\rangle \langle \alpha_k|), \mathcal{S}_1(|\alpha_k\rangle \langle \alpha_k|)] &:= \prod_{k=1}^M F_k, \end{aligned} \quad (69)$$

where  $F_k$  is the fidelity between the two single-mode Gaussian states  $\mathcal{S}_0(|\alpha_k\rangle \langle \alpha_k|)$  and  $\mathcal{S}_1(|\alpha_k\rangle \langle \alpha_k|)$ . In order to compute  $F_k$ , let us consider the explicit action of  $\mathcal{S}_u$  on the coherent state  $|\alpha_k\rangle \langle \alpha_k|$ , which is a Gaussian state with CM  $\mathbf{V} = \mathbf{I}$  and displacement  $\bar{\mathbf{x}}^T = (2\text{Re}(\alpha_k), 2\text{Im}(\alpha_k))$ . At the output of  $\mathcal{S}_u$ , we get a Gaussian state  $\mathcal{S}_u(|\alpha_k\rangle \langle \alpha_k|)$  whose statistical moments are proportional to the input ones, i.e.,  $\mathbf{V}_u = \xi_u \mathbf{I}$  and  $\bar{\mathbf{x}}_u = \sqrt{r_u} \bar{\mathbf{x}}$ , were  $\xi_u$  is given in Eq. (64). Notice that  $\xi_u \geq 1$  because  $\mathbf{V}_u$  must be a bona-fide CM [32]. Then, by using the formula of Ref. [42], we can compute the analytical expression of the fidelity, which is equal to

$$F_k = \omega^{-1} \exp[-\lambda |\alpha_k|^2], \quad (70)$$

where  $\omega$  and  $\lambda$  are defined in Eqs. (62) and (63), respectively. It is trivial to check that  $\omega \geq 1$  and  $\lambda \geq 0$  using  $\xi_u \geq 1$ . Now, using Eq. (70) into Eq. (69), we get

$$F[\sigma_0(\boldsymbol{\alpha}), \sigma_1(\boldsymbol{\alpha})] = \omega^{-M} \exp \left[ -\lambda \sum_{k=1}^M |\alpha_k|^2 \right] = g(E), \quad (71)$$

where

$$g(E) := \omega^{-M} \exp[-\lambda E], \quad (72)$$

and  $E$  is defined in Eq. (54). Thus, by combining Eqs. (66), (68) and (71), we get

$$D(\sigma_0, \sigma_1) \leq \mathcal{I} := \int d^{2M} \boldsymbol{\alpha} \mathcal{P}(\boldsymbol{\alpha}) \mathcal{B}(E), \quad (73)$$

where we have introduced the  $\mathbb{R}^+ \rightarrow [0, 1]$  function

$$\mathcal{B}(E) := \sqrt{1 - g(E)}. \quad (74)$$

Since the latter quantity depends only on the real scalar  $E$ , we can greatly simplify the integral  $\mathcal{I}$  in Eq. (73). For this sake, let us introduce the polar coordinates

$$\boldsymbol{\alpha} = \sqrt{\mathbf{e}} \exp(i\boldsymbol{\theta}), \quad (75)$$

where  $\mathbf{e} := (e_1, \dots, e_M)$  is a vector with generic element  $e_k := |\alpha_k|^2$ , and  $\boldsymbol{\theta} := (\theta_1, \dots, \theta_M)$  is a vector of phases (here  $d^{2M} \boldsymbol{\alpha} = 2^{-M} d^M \mathbf{e} d^M \boldsymbol{\theta}$ ). Then, we can write

$$\mathcal{I} = \int_0^{+\infty} d^M \mathbf{e} \mathcal{R}(\mathbf{e}) \mathcal{B}(E), \quad (76)$$

where  $\mathcal{R}(\mathbf{e})$  is the radial probability distribution

$$\mathcal{R}(\mathbf{e}) := \int_0^{2\pi} \frac{d^M \boldsymbol{\theta}}{2^M} \mathcal{P}(\mathbf{e}, \boldsymbol{\theta}), \quad (77)$$

and

$$\mathcal{P}(\mathbf{e}, \boldsymbol{\theta}) := [\mathcal{P}(\boldsymbol{\alpha})]_{\boldsymbol{\alpha}=\sqrt{\mathbf{e}} \exp(i\boldsymbol{\theta})}. \quad (78)$$

The integral can be further simplified by setting

$$e_M = E - \sum_{k=1}^{M-1} e_k, \quad (79)$$

which introduces the further change of variables

$$\mathbf{e} \rightarrow \mathbf{e}' := (e_1, \dots, e_{M-1}, E). \quad (80)$$

Then, we get

$$\mathcal{I} = \int_0^{+\infty} dE \mathcal{R}(E) \mathcal{B}(E), \quad (81)$$

where

$$\begin{aligned} \mathcal{R}(E) &:= \int_0^E de_1 \int_0^{E-e_1} de_2 \times \\ &\dots \times \int_0^{E-\sum_{k=1}^{M-2} e_k} de_{M-1} \mathcal{R}(\mathbf{e}'), \end{aligned} \quad (82)$$

and

$$\mathcal{R}(\mathbf{e}') := [\mathcal{R}(\mathbf{e})]_{e_M=E-\sum_{k=1}^{M-1} e_k}. \quad (83)$$

It is clear that the simplification of the integral from Eq. (73) to Eq. (81) can be done not just for  $\mathcal{B}(E)$ , but for a generic integrable function  $f(E)$ . As a consequence, we can repeat the same simplification for  $f(E) = E$ , which corresponds to write the following expression for the total number of photons

$$N = \int_0^{+\infty} dE \mathcal{R}(E) E. \quad (84)$$

Analytically, it is easy to check that  $\mathcal{B}(E)$  is concave, i.e.,

$$p\mathcal{B}(E) + (1-p)\mathcal{B}(E') \leq \mathcal{B}[pE + (1-p)E'], \quad (85)$$

for every  $E, E' \in \mathbb{R}^+$  and  $p \in [0, 1]$ . Then, applying Jensen's inequality [43], we get

$$\begin{aligned} \mathcal{I} &\leq \mathcal{B} \left[ \int_0^{+\infty} dE \mathcal{R}(E) E \right] = \mathcal{B}(N) \\ &= \sqrt{1 - g(N)}. \end{aligned} \quad (86)$$

Here we can set

$$g(N) = F(n_S)^M, \quad (87)$$

where  $n_S = N/M$  and  $F(n_S)$  is given in Eq. (61). According to Eq. (70),  $F(n_S)$  represents the fidelity between the two states  $\mathcal{S}_0(|\sqrt{n_S}\rangle\langle\sqrt{n_S}|)$  and  $\mathcal{S}_1(|\sqrt{n_S}\rangle\langle\sqrt{n_S}|)$ , i.e., the two possible outputs of the coherent state  $|\sqrt{n_S}\rangle$ . In conclusion, by combining Eqs. (73), (86) and (87), we get

$$D(\sigma_0, \sigma_1) \leq \sqrt{1 - F(n_S)^M}. \quad (88)$$

Using the latter equation with Eq. (65), we obtain the lower bound of Eq. (60). ■

According to the previous theorem, the classical discrimination bound  $\mathcal{C}(M, N)$  can be *computed* by assuming a coherent-state transmitter which signals  $M$  identical coherent states with  $n_S = N/M$  mean photons each. This transmitter can be denoted by

$$T_{coh} = T(M, 0, |\sqrt{n_S}\rangle\langle\sqrt{n_S}|^{\otimes M}), \quad (89)$$

and is schematically depicted in Fig. 10. Despite the computation of  $\mathcal{C}(M, N)$  can be performed in this simple way, we do not know which classical transmitter is actually able to reach, or approach, the lower bound  $\mathcal{C}(M, N)$ .

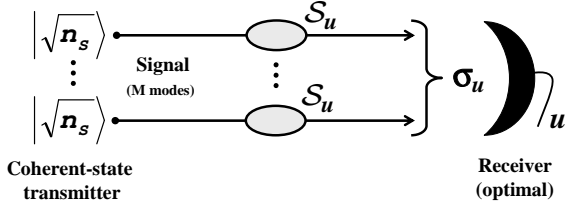


FIG. 10: Coherent-state transmitter which signals  $M$  copies of a coherent state  $|\sqrt{n_s}\rangle$  with mean photon number  $n_s$ .

### B. Pure-loss model

For the pure-loss model of Fig. 7, the previous theorem can be greatly simplified. In particular, we get a classical discrimination bound which does not depend on the bandwidth  $M$ , but only on the total energy  $N$  of the signal. This result is stated in the following corollary (which corresponds to the first theorem in our Letter).

**Corollary 5** *Let us consider the discrimination of two attenuator channels,  $\mathcal{E}_0 = \mathcal{E}(r_0)$  and  $\mathcal{E}_1 = \mathcal{E}(r_1)$ , by using a classical transmitter  $T_c = T(M, L, \rho_c)$  which signals  $N$  photons. Then, we have*

$$P_{err}(\mathcal{E}_0 \neq \mathcal{E}_1 | T_c) \geq \mathcal{C}(N), \quad (90)$$

where

$$\mathcal{C}(N) := \frac{1 - \sqrt{1 - \exp[-N(\sqrt{r_1} - \sqrt{r_0})^2]}}{2}. \quad (91)$$

**Proof.** Let us set  $\bar{n} = \varepsilon = 0$  in Theorem 4, so that

$$\begin{aligned} \mathcal{G}_u &= \mathcal{S}_u \otimes \mathcal{D} = [\mathcal{N}(0) \circ \mathcal{E}(r_u, 0) \circ \mathcal{N}(0)] \otimes [\mathcal{N}(0) \circ \mathcal{N}(0)] \\ &= [\mathcal{I} \circ \mathcal{E}(r_u) \circ \mathcal{I}] \otimes [\mathcal{I} \circ \mathcal{I}] = \mathcal{E}_u \otimes \mathcal{I}. \end{aligned} \quad (92)$$

Clearly we can write  $P_{err}(\mathcal{G}_0 \neq \mathcal{G}_1 | T_c) = P_{err}(\mathcal{E}_0 \neq \mathcal{E}_1 | T_c)$ . This quantity is lower-bounded by using Eq. (60) where now the fidelity term  $F(n_s)^M$  can be greatly simplified. In fact, because of  $\bar{n} = \varepsilon = 0$ , here we have  $\xi_u = 1$ , which implies

$$\omega = 1, \quad \lambda = (\sqrt{r_0} - \sqrt{r_1})^2. \quad (93)$$

As a consequence, we have

$$\begin{aligned} F(n_s)^M &= \left\{ \exp[-n_s(\sqrt{r_1} - \sqrt{r_0})^2] \right\}^M \\ &= \exp[-N(\sqrt{r_1} - \sqrt{r_0})^2], \end{aligned} \quad (94)$$

providing the expression of Eq. (91). ■

## IV. QUANTUM TRANSMITTER

As explained in the Letter, we consider a particular kind of non-classical transmitter, that we call ‘‘EPR transmitter’’. This is given by

$$T_{ep\!r} = T(M, M, |\xi\rangle \langle \xi|^{\otimes M}), \quad (95)$$

where  $|\xi\rangle$  is the TMSV state described in Sec. I. This transmitter is completely characterized by the basic parameters of the emitted signal, i.e., bandwidth  $M$  and energy  $N$ , since  $N = Mn_s = M \sinh^2 \xi$ . For this reason, we also use the notation  $T_{ep\!r} = T_{M,N}$ . Given this transmitter, we now show how to compute the error probability which affects the channel discrimination. We consider the general case of the thermal-loss model, but it is understood that the results hold for the pure-loss model by setting  $\bar{n} = \varepsilon = 0$ .

Given an arbitrary EPR transmitter, the corresponding input state

$$\rho = |\xi\rangle \langle \xi|^{\otimes M}, \quad (96)$$

is transformed into the conditional output state

$$\sigma_u = \varphi_u^{\otimes M}, \quad (97)$$

where

$$\varphi_u = \mathcal{G}_u(|\xi\rangle \langle \xi|) = (\mathcal{S}_u \otimes \mathcal{D})(|\xi\rangle \langle \xi|). \quad (98)$$

The single-copy output state  $\varphi_u$  has zero mean and its CM  $\mathbf{V}_u$  can be easily computed from the one of the TMSV state, which is given in Eq. (10). In fact, if we write the bipartite channel

$$\mathcal{S}_u \otimes \mathcal{D} = [\mathcal{N}(\varepsilon) \circ \mathcal{E}(r_u, \bar{n}) \circ \mathcal{N}(\varepsilon)] \otimes \mathcal{N}(2\varepsilon) \quad (99)$$

in terms of  $(\mathbf{K}, \mathbf{N})$  matrices by using Eqs. (18) and (19), we can exploit the result of Eq. (21). Thus, we get the output CM

$$\mathbf{V}_u = \begin{pmatrix} [r_u(\mu + \varepsilon) + (1 - r_u)\beta + \varepsilon]\mathbf{I} & \sqrt{r_u(\mu^2 - 1)}\mathbf{Z} \\ \sqrt{r_u(\mu^2 - 1)}\mathbf{Z} & (\mu + 2\varepsilon)\mathbf{I} \end{pmatrix}, \quad (100)$$

where

$$\mu := 2n_s + 1, \quad \beta := 2\bar{n} + 1. \quad (101)$$

Now, the error probability which affects the channel discrimination  $P_{err}(\mathcal{G}_0 \neq \mathcal{G}_1 | T_{M,N})$  is equal to the minimum error probability in the  $M$ -copy discrimination between  $\varphi_0$  and  $\varphi_1$ . This quantity is upper-bounded by the quantum Chernoff bound, i.e.,

$$P_{err}(\mathcal{G}_0 \neq \mathcal{G}_1 | T_{M,N}) \leq \mathcal{Q}(M, N). \quad (102)$$

where

$$\mathcal{Q}(M, N) = \frac{1}{2} \left[ \inf_{t \in (0,1)} \text{Tr}(\varphi_0^t \varphi_1^{1-t}) \right]^M. \quad (103)$$

To compute  $\mathcal{Q}(M, N)$  we perform the normal-mode decomposition of the Gaussian states  $\varphi_0$  and  $\varphi_1$ , which corresponds to the symplectic decomposition of the conditional CM of Eq. (100) [14, 32]. Then, we apply the symplectic formula of Ref. [14]. Unfortunately, the result is extremely long to be presented here (but short analytical expressions are provided afterwards in the proofs for the pure-loss model). Note that an alternative upper-bound is the quantum Battacharyya bound, which is given by

$$\mathcal{B}(M, N) = \frac{1}{2} \left[ \text{Tr} \left( \varphi_0^{1/2} \varphi_1^{1/2} \right) \right]^M \geq \mathcal{Q}(M, N). \quad (104)$$

This bound is larger but generally easier to compute than the quantum Chernoff bound (see Ref. [14] for details).

## V. QUANTUM-CLASSICAL COMPARISON

In this section we show how to make the comparison between the EPR transmitter and the classical transmitters in order to reply to the basic questions of Eqs. (38) and (45). Our strategy is to derive a sufficient condition for the superiority of the EPR transmitter by comparing the bounds derived in the previous sections. On the one hand, we know that the error probability of any classical transmitter  $P_{err}^{class}$  is lower-bounded by  $\mathcal{C}$ . On the other hand, the error probability of the EPR transmitter  $P_{err}^{epr}$  is upper-bound by  $\mathcal{Q}$ . Thus, a sufficient condition for  $P_{err}^{epr} < P_{err}^{class}$  is provided by the inequality  $\mathcal{Q} < \mathcal{C}$ . Depending on the model, our answer can be analytical or numerical.

### A. Pure-loss model

For the pure-loss model, we have  $\mathcal{Q} = \mathcal{Q}(M, N)$  and  $\mathcal{C} = \mathcal{C}(N)$ . Since here the classical discrimination bound is not dependent on the bandwidth, it is sufficient to find a  $\bar{M}$  such that  $\mathcal{Q}(\bar{M}, N) < \mathcal{C}(N)$ . In other words, our basic question of Eq. (38) becomes the following: given two channels  $\{\mathcal{E}_0, \mathcal{E}_1\}$  and signal-energy  $N$ , can we find a bandwidth  $\bar{M}$  such that

$$\mathcal{Q}(\bar{M}, N) < \mathcal{C}(N) ? \quad (105)$$

This clearly implies the existence of an EPR transmitter  $T_{\bar{M}, N}$  such that

$$P_{err}(\mathcal{E}_0 \neq \mathcal{E}_1 | T_{\bar{M}, N}) < P_{err}(\mathcal{E}_0 \neq \mathcal{E}_1 | T_c), \quad (106)$$

for every  $T_c$ . As stated in our Letter this question has a positive answer, and this is provided by our “threshold energy” theorem. According to this theorem, for every pair of attenuator channels  $\{\mathcal{E}_0, \mathcal{E}_1\}$  and above a threshold energy  $N_{th}$ , there is an EPR transmitter (with suitable bandwidth  $\bar{M}$ ) which outperforms any classical transmitter. Furthermore, we can prove a stronger result if one of the two channels is just the identity, e.g.,

we have  $\{\mathcal{E}_0, \mathcal{I}\}$ . In this case we have  $N_{th} = 1/2$  and  $\bar{M}$  is a minimum bandwidth, as stated by the “ideal memory” theorem in our Letter. We give the explicit proofs of these theorems in Sec. VI.

In order to quantify numerically the advantage brought by the EPR transmitter, we introduce the minimum information gain

$$G := 1 - H(\mathcal{Q}) - [1 - H(\mathcal{C})] = G(M, N), \quad (107)$$

where

$$H(x) := -x \log_2 x - (1-x) \log_2 (1-x) \quad (108)$$

is the binary Shannon entropy. Finding a bandwidth  $\bar{M}$  such that  $G(\bar{M}, N) > 0$  clearly implies the validity of Eq. (106). In terms of memory readout, this quantity lowerbounds the number of bits per cell which are gained by an EPR transmitter  $T_{\bar{M}, N}$  over any classical transmitter. By using  $G$  one can perform extensive numerical investigations [44]. In particular, one can check that narrowband EPR transmitters (i.e., with low  $\bar{M}$ ) are able to give  $G > 0$  in the regime of few photons  $N$  and high-reflectivities (i.e.,  $r_0$  or  $r_1$  sufficiently close to 1). These numerical results are shown and discussed in Fig. 2(left) and Fig. 3 of our Letter.

### B. Thermal-loss model

For the thermal-loss model, we have  $\mathcal{Q} = \mathcal{Q}(M, N)$  and  $\mathcal{C} = \mathcal{C}(M, N)$ . Here the classical discrimination bound  $\mathcal{C}$  depends on the bandwidth  $M$  and tends monotonically to zero for  $M \rightarrow \infty$ . This is evident from the general expression of the fidelity term  $F(n_S)^M$  which is present in Eq. (60). In fact, from Eq. (61), we get

$$F(n_S)^M = \omega^{-M} \exp(-\lambda N), \quad (109)$$

which decreases to zero for  $M \rightarrow \infty$  whenever  $\omega > 1$  (as is generally the case for the thermal-loss model). For this reason, let us fix a maximum bandwidth  $M^*$  and consider the minimum value

$$\inf_{M \in [1, M^*]} \mathcal{C}(M, N) = \mathcal{C}(M^*, N). \quad (110)$$

It is clear that, given two bipartite channels  $\{\mathcal{G}_0, \mathcal{G}_1\}$  and signal-energy  $N$ , we have

$$P_{err}(\mathcal{G}_0 \neq \mathcal{G}_1 | T_c) \geq \mathcal{C}(M^*, N), \quad (111)$$

for every  $T_c = T(M, L, \rho_c)$  with signal-bandwidth  $M \leq M^*$ . In other words, using  $\mathcal{C}(M^*, N)$  we can bound all the classical transmitters up to the maximum bandwidth  $M^*$ . As a result, our basic question of Eq. (45) becomes the following: given two bipartite channels  $\{\mathcal{G}_0, \mathcal{G}_1\}$  and signal-energy  $N$ , can we find an EPR transmitter with suitable bandwidth  $\bar{M}$  such that

$$\mathcal{Q}(\bar{M}, N) < \mathcal{C}(M^*, N) ? \quad (112)$$

This clearly implies the existence of an EPR transmitter  $T_{\bar{M},N}$  such that

$$P_{err}(\mathcal{G}_0 \neq \mathcal{G}_1 | T_{\bar{M},N}) < P_{err}(\mathcal{G}_0 \neq \mathcal{G}_1 | T_c), \quad (113)$$

for every  $T_c = T(M, L, \rho_c)$  with  $M \leq M^*$ . As explicitly discussed in the Letter, this question has a positive answer too, and the value of  $M^*$  can be so high to include all the classical transmitters which are physically meaningful for the memory model. However, despite the previous case, here the answer can only be numerical. In fact, the two bipartite channels  $\{\mathcal{G}_0, \mathcal{G}_1\}$  are characterized by four parameters  $\{r_0, r_1, \bar{n}, \varepsilon\}$  and the comparison between transmitters involves further three parameters  $\{\bar{M}, M^*, N\}$ . For this reason, the explicit expression of the minimum information gain now depends on seven parameters, i.e.,

$$G = G(\bar{M}, M^*, N, r_0, r_1, \bar{n}, \varepsilon). \quad (114)$$

By performing numerical investigations, one can analyze the positivity of  $G$ , which clearly implies the condition of Eq. (113). According to Fig. 2(right) of our Letter, we can achieve remarkable positive gains when we compare narrowband EPR transmitters (low  $\bar{M}$ ) with wide sets of classical transmitters (large  $M^*$ ) in the regime of few photons (low  $N$ ) and high reflectivities ( $r_0$  or  $r_1$  close to 1), and assuming the presence of non-trivial decoherence (e.g.,  $\varepsilon = \bar{n} = 10^{-5}$ ). See the Letter for physical discussions.

## VI. ANALYTICAL RESULTS FOR THE PURE-LOSS MODEL

In this section we provide the detailed proofs of the two theorems relative to the pure-loss model: the ‘‘threshold energy’’ theorem and the ‘‘ideal memory’’ theorem. Given two attenuator channels,  $\mathcal{E}_0 = \mathcal{E}(r_0)$  and  $\mathcal{E}_1 = \mathcal{E}(r_1)$ , and given the total signal-energy  $N$ , the basic problem is to show the existence of an EPR transmitter  $T_{M,N}$  which is able to beat the classical discrimination bound  $\mathcal{C}(N)$ , and, therefore, all the classical transmitters  $T_c$ . The two theorems provide sufficient conditions for the existence of this quantum transmitter.

### A. ‘‘Threshold energy’’ theorem

For the sake of completeness we repeat here the statement of the theorem (this is perfectly equivalent to the statement provided in our Letter).

**Theorem 6** *Let us consider the discrimination of two attenuator channels,  $\mathcal{E}_0 = \mathcal{E}(r_0)$  and  $\mathcal{E}_1 = \mathcal{E}(r_1)$  with  $r_0 \neq r_1$ , by using transmitters with (finite) signal energy*

$$N > N_{th}(r_0, r_1) := \frac{2 \ln 2}{2 - r_0 - r_1 - 2\sqrt{(1-r_0)(1-r_1)}}. \quad (115)$$

*Then, there exists an EPR transmitter  $T_{\bar{M},N}$ , with suitable bandwidth  $\bar{M}$ , such that*

$$P_{err}(\mathcal{E}_0 \neq \mathcal{E}_1 | T_{\bar{M},N}) < \mathcal{C}(N). \quad (116)$$

**Proof.** For simplicity, in this proof we use the shorthand notation  $P_{err}(T) := P_{err}(\mathcal{E}_0 \neq \mathcal{E}_1 | T)$ . According to Corollary 5, the error probability for an arbitrary classical transmitter  $T_c$  is lower-bounded by the classical discrimination bound, i.e.,  $P_{err}(T_c) \geq \mathcal{C}(N)$ , where  $\mathcal{C}(N)$  is given in Eq. (91). Note that, for every  $z \in [0, 1]$ , we have

$$\frac{1 - \sqrt{1-z}}{2} \geq \frac{z}{4}. \quad (117)$$

As a consequence, we can write

$$\mathcal{C}(N) \geq \frac{e^{-Nx^2}}{4} := \tilde{\mathcal{C}}(N), \quad (118)$$

where

$$x := \sqrt{r_1} - \sqrt{r_0}. \quad (119)$$

Now let us consider an EPR transmitter  $T_{M,N}$ . The corresponding error probability  $P_{err}(T_{M,N})$  can be upper-bounded via the quantum Battacharyya bound  $\mathcal{B}(M, N)$  defined in Eq. (104). This bound can be computed from the conditional CM of Eq. (100) by setting  $\bar{n} = \varepsilon = 0$  (see Sec. IV and Ref. [14]). In this problem, for fixed (finite) energy  $N$ , the bound  $\mathcal{B}(M, N)$  is not monotonic in  $M$  (easy to check numerically). However, it is regular in  $M$  and its asymptotic limit  $\mathcal{B}_\infty(N) := \lim_{M \rightarrow +\infty} \mathcal{B}(M, N)$  exists. In particular, the asymptotic Battacharyya bound is equal to

$$\mathcal{B}_\infty(N) = \frac{e^{-Nw}}{2}, \quad (120)$$

where  $w \in [0, 3/2]$  is defined by

$$w := \frac{r_0 + r_1 + 2}{2} - 2\sqrt{r_0 r_1} - \sqrt{(1-r_0)(1-r_1)}. \quad (121)$$

Clearly we have

$$\inf_M P_{err}(T_{M,N}) \leq \inf_M \mathcal{B}(M, N) \leq \mathcal{B}_\infty(N), \quad (122)$$

which means that  $\forall \varepsilon > 0, \exists \bar{M} \in \mathbb{Z}^+$  such that

$$P_{err}(T_{\bar{M},N}) < \mathcal{B}_\infty(N) + \varepsilon. \quad (123)$$

In order to prove the result, let us impose the threshold condition

$$\mathcal{B}_\infty(N) < \tilde{\mathcal{C}}(N). \quad (124)$$

Now, if Eq. (124) is satisfied, then we can always take an  $\varepsilon > 0$  such that

$$\tilde{\mathcal{C}}(N) = \mathcal{B}_\infty(N) + \varepsilon. \quad (125)$$

Then, because of the proposition of Eq. (123), we have that  $\exists \bar{M} \in \mathbb{Z}^+$  such that

$$P_{err}(T_{\bar{M},N}) < \tilde{\mathcal{C}}(N) \leq \mathcal{C}(N) . \quad (126)$$

For this reason, the next step is to solve Eq. (124) in order to get a threshold condition on the energy  $N$ . It is easy to check that, by using Eqs. (118)-(121), the condition of Eq. (124) becomes

$$Nf > 1 , \quad (127)$$

where

$$f := \frac{w - x^2}{\ln 2} = \frac{1}{\ln 2} \left[ \frac{(1-r_0) + (1-r_1)}{2} - \sqrt{(1-r_0)(1-r_1)} \right] . \quad (128)$$

Since  $f$  is proportional to the difference between an arithmetic mean and a geometric mean, we have  $f \geq 0$ , and  $f = 0$  if and only if  $r_0 = r_1$ . Thus, if we exclude the singular case  $r_0 = r_1$ , we can write

$$N > \frac{1}{f} = N_{th}(r_0, r_1) . \quad (129)$$

In conclusion, if the threshold condition of Eq. (129) is satisfied (where  $r_0 \neq r_1$ ), then there exists a bandwidth  $\bar{M}$  such that  $P_{err}(T_{\bar{M},N}) < \mathcal{C}(N)$ . ■

## B. “Ideal memory” theorem

Here we prove the ideal memory theorem which refers to the case of ideal memories, i.e., having  $r_0 < r_1 = 1$ . This scenario corresponds to discriminating between an attenuator channel  $\mathcal{E}(r_0)$  and the identity channel  $\mathcal{I} = \mathcal{E}(1)$ . For this reason, the quantum Chernoff bound  $\mathcal{Q}(M, N)$  has a simple analytical expression, which turns out to be decreasing in  $M$  (for fixed energy  $N$ ). Thanks to this monotony, our result can be proven above a minimum bandwidth  $\bar{M}$ . In fact,  $\mathcal{Q}(M, N)$  decreasing in  $M$  implies that  $G = 1 - H[\mathcal{Q}(M, N)] - \{1 - H[\mathcal{C}(N)]\}$  is increasing in  $M$ , so that optimal gains are monotonically reached by broadband EPR transmitters. Note that this was not possible to prove for the previous theorem (see Sec. VI A) since, in that case, the quantum Battacharyya bound  $\mathcal{B}(M, N)$  turned out to be non-monotonic in  $M$ .

For the sake of completeness we repeat here the statement of the “ideal memory” theorem (this is perfectly equivalent to the statement provided in our Letter).

**Theorem 7** *Let us consider the discrimination of an attenuator channel  $\mathcal{E}_0 = \mathcal{E}(r_0)$ , with  $r_0 < 1$ , from the identity channel  $\mathcal{I}$ , by using transmitters with signal energy*

$$N \geq N_{th} := 1/2 . \quad (130)$$

*Then, there exists a minimum bandwidth  $\bar{M}$  such that, for every EPR transmitter  $T_{M,N}$  with  $M > \bar{M}$ , we have*

$$P_{err}(\mathcal{E}_0 \neq \mathcal{I}|T_{M,N}) < \mathcal{C}(N) . \quad (131)$$

**Proof.** Given the discrimination problem  $\mathcal{E}_0 \neq \mathcal{I}$  for fixed signal energy  $N$ , let us consider an EPR transmitter  $T_{M,N}$ . Its error probability  $P_{err}(T_{M,N}) = P_{err}(\mathcal{E}_0 \neq \mathcal{I}|T_{M,N})$  is upper-bounded by the quantum Chernoff bound  $\mathcal{Q}(M, N)$ , whose analytical expression is greatly simplified here. In fact, we have

$$\mathcal{Q}(M, N) = \frac{1}{2} \left( 1 + \frac{N}{M} x \right)^{-2M} , \quad (132)$$

where

$$x = 1 - \sqrt{r_0} \in (0, 1] . \quad (133)$$

This expression can be computed using the procedure sketched in Sec. IV by setting  $\bar{n} = \varepsilon = 0$  and  $r_1 = 1$  in the conditional CM of Eq. (100). For fixed energy  $N$ , it is very easy to check analytically that  $\mathcal{Q}(M, N)$  is decreasing in  $M$  (strictly decreasing if we exclude the trivial case  $N = 0$ ). Since  $\mathcal{Q}$  is bounded ( $\mathcal{Q} \in [0, 1/2]$ ) and decreasing in  $M$ , the broadband limit

$$\mathcal{Q}_\infty(N) := \lim_{M \rightarrow +\infty} \mathcal{Q}(M, N) \quad (134)$$

exists, and clearly coincides with the infimum, i.e.,

$$\mathcal{Q}_\infty(N) = \inf_M \mathcal{Q}(M, N) . \quad (135)$$

Explicitly, we compute

$$\mathcal{Q}_\infty(N) = \frac{1}{2} \exp(-2Nx) . \quad (136)$$

By definition of limit, Eqs. (134) and (135) mean that  $\forall \varepsilon > 0, \exists \bar{M} \in \mathbb{Z}^+$  such that  $\forall M > \bar{M}$

$$\mathcal{Q}_\infty(N) \leq \mathcal{Q}(M, N) < \mathcal{Q}_\infty(N) + \varepsilon . \quad (137)$$

Now, since we have  $P_{err}(T_{M,N}) \leq \mathcal{Q}(M, N)$  for every  $M$ , it is clear that  $\forall \varepsilon > 0, \exists \bar{M} \in \mathbb{Z}^+$  such that  $\forall M > \bar{M}$

$$P_{err}(T_{M,N}) < \mathcal{Q}_\infty(N) + \varepsilon . \quad (138)$$

In order to prove our result, we impose the threshold condition

$$\mathcal{Q}_\infty(N) < \mathcal{C}(N) , \quad (139)$$

where  $\mathcal{C}(N)$  is the classical discrimination bound. According to Corollary 5, this is given by

$$\mathcal{C}(N) = \frac{1 - \sqrt{1 - z}}{2} , \quad (140)$$

where

$$z = \exp(-Nx^2) . \quad (141)$$

Now, if Eq. (139) is satisfied, then we can always take an  $\varepsilon > 0$  such that

$$\mathcal{C}(N) = \mathcal{Q}_\infty(N) + \varepsilon . \quad (142)$$

Then, because of the proposition of Eq. (138), we have that  $\exists \bar{M} \in \mathbb{Z}^+$  such that  $\forall M > \bar{M}$

$$P_{err}(T_{M,N}) < \mathcal{C}(N) . \quad (143)$$

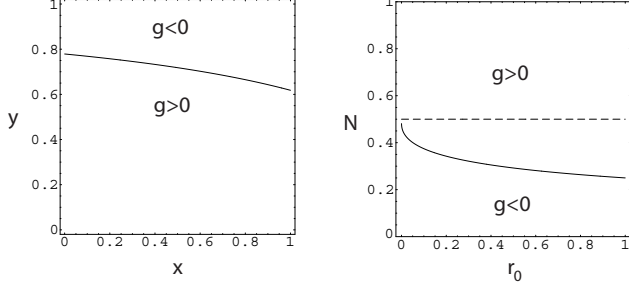


FIG. 11: **Left.** Zero-level function  $\bar{y}(x)$  plotted in the finite  $(x, y)$ -plane. Only for  $y < \bar{y}(x)$  we have  $g(x, y) > 0$ . **Right.** Energy function  $\bar{N}(r_0)$  plotted in the infinite  $(r_0, N)$ -plane (here restricted to the sector  $0 < N \leq 1$ ). Only for  $N > \bar{N}(r_0)$  we have  $g = g(r_0, N) > 0$ . Dashed line corresponds to the universal energy threshold  $N_{th} = 1/2$ .

Clearly, the next step is to solve Eq. (139) and get a threshold condition on the energy  $N$ . After simple Algebra, Eq. (139) can be written as

$$g(x, y) > 0 , \quad (144)$$

where

$$g(x, y) := y^{x^2} + y^{4x} - 2y^{2x} , \quad (145)$$

and

$$y := \exp(-N) \in (0, 1) . \quad (146)$$

Note that, in the definition of  $y$ , we are excluding the singular points  $N = 0, +\infty$ . The function  $g(x, y)$  can be easily analyzed on the plane  $(0, 1] \times (0, 1)$ . In particular, its zero-level  $g(x, y) = 0$  is represented by the continuous function  $\bar{y}(x)$  which is plotted in Fig. 11(left). The threshold condition of Eq. (144) is equivalent to

$$y < \bar{y}(x) . \quad (147)$$

As evident from Fig. 11(left), the function  $\bar{y}(x)$  is decreasing in  $x \in (0, 1]$  with extremal values

$$\lim_{x \rightarrow 0^+} \bar{y}(x) = \sup_{x \in (0, 1]} \bar{y}(x) = e^{-1/4} , \quad (148)$$

and

$$\lim_{x \rightarrow 1^-} \bar{y}(x) = \bar{y}(1) = \min_{x \in (0, 1]} \bar{y}(x) = \frac{\sqrt{5} - 1}{2} . \quad (149)$$

Equivalently, by using Eqs. (133) and (146), we can put the threshold condition of Eq. (147) in terms of  $r_0$  and  $N$ . In particular, Eq. (147) takes the form

$$N > \bar{N}(r_0) , \quad (150)$$

where  $\bar{N}(r_0)$  is the decreasing function of  $r_0 \in [0, 1)$  which is plotted in Fig. 11(right). This function has extremal values

$$\bar{N}(0) = \max_{r_0 \in [0, 1)} \bar{N}(r_0) = \ln \frac{2}{\sqrt{5} - 1} , \quad (151)$$

and

$$\lim_{r_0 \rightarrow 1^-} \bar{N}(r_0) = \inf_{r_0 \in [0, 1)} \bar{N}(r_0) = \frac{1}{4} . \quad (152)$$

In order to have a criterion which is universal, i.e.,  $r_0$ -independent, we can consider the sufficient condition

$$N > \max_{r_0 \in [0, 1)} \bar{N}(r_0) = \ln \frac{2}{\sqrt{5} - 1} \simeq 0.48 , \quad (153)$$

which clearly implies Eq. (150). More easily we can consider the slightly-larger condition

$$N \geq N_{th} := 1/2 . \quad (154)$$

In conclusion, for every  $r_0 < r_1 = 1$  and (finite)  $N \geq N_{th} := 1/2$ , there exists a minimum bandwidth  $\bar{M}$  such that  $\forall M > \bar{M}$  we have  $P_{err}(T_{M,N}) < \mathcal{C}(N)$ . ■

## VII. SUB-OPTIMAL RECEIVER

In our derivations we have assumed that the output receiver is able to perform an optimal measurement given by the ‘‘Helstrom’s POVM’’ of Eq. (32). Despite this measurement has an extremely simple formula, it is not straightforward to implement it using linear optics and photodetection. This problem has been already considered in Ref. [9] for the case of quantum illumination, where an ingenious receiver design has been proven to harness quantum illumination advantage. Unfortunately this kind of design cannot be applied directly to our scheme, since quantum reading not only has a different task than quantum illumination but also works in a completely different regime (high reflectivities, low thermal-noise and narrowband signals). Note that the working regime of quantum reading is such that strong correlations survive at the output of the process. For this reason, we can consider simpler receiver designs than the ones for quantum illumination. In fact, here we prove that an output Bell detection followed by a simple classical processing is a sub-optimal receiver able to provide remarkable advantages, i.e., comparable to the Helstrom’s POVM. Since Bell detection is a standard measurement (involving linear optics and photodetection) our reading apparatus can be easily implemented in today’s quantum optics labs.



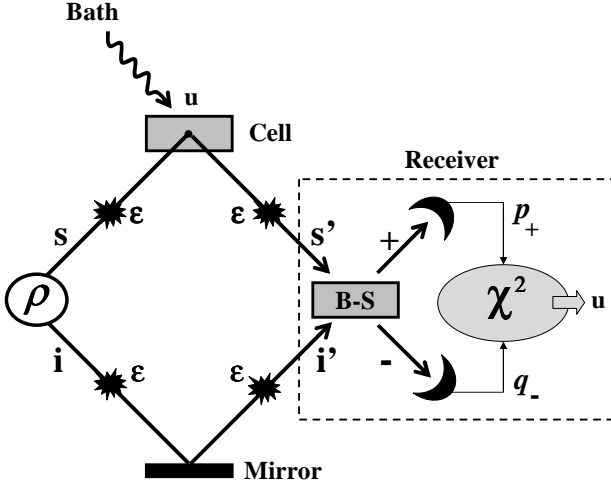


FIG. 12: Quantum reading scheme with sub-optimal receiver. This receiver consists of two parts. The first part is a Bell measurement, which consists in a balanced beam-splitter followed by two homodyne detectors. The second part is a classical processing of the outcome  $\{q_-, p_+\}$  by means of a  $\chi^2$ -test. See text for more details.

The quantum reading scheme with the sub-optimal receiver is depicted in Fig. 12. The input modes  $\{s, i\}$  belong to a TMSV state  $\rho = |\xi\rangle\langle\xi|$ . These modes are processed as usual, i.e., the signal mode  $s$  is conditionally transformed by the cell (reflectivity  $r_u$  encoding the bit  $u$ ) while the idler mode  $i$  is sent directly to the receiver. Their quadratures,  $\hat{\mathbf{x}}_s = (\hat{q}_s, \hat{p}_s)^T$  and  $\hat{\mathbf{x}}_i = (\hat{q}_i, \hat{p}_i)^T$ , are transformed according to the input-output relations

$$\hat{\mathbf{x}}_s \rightarrow \hat{\mathbf{x}}_{s'} = \sqrt{r_u}(\hat{\mathbf{x}}_s + \hat{\mathbf{x}}_\varepsilon) + \sqrt{1-r_u}\hat{\mathbf{x}}_b + \hat{\mathbf{x}}'_\varepsilon, \quad (155)$$

and

$$\hat{\mathbf{x}}_i \rightarrow \hat{\mathbf{x}}_{i'} = \hat{\mathbf{x}}_i + 2\hat{\mathbf{x}}''_\varepsilon, \quad (156)$$

where  $\hat{\mathbf{x}}_b$  are the quadratures of the external thermal bath, while  $\hat{\mathbf{x}}_\varepsilon$ ,  $\hat{\mathbf{x}}'_\varepsilon$  and  $\hat{\mathbf{x}}''_\varepsilon$  are quadratures associated with the internal thermal channels. At the receiver the two modes  $\{s', i'\}$  are combined in a balanced beam-splitter which outputs the modes  $\{-, +\}$  with quadratures

$$\hat{\mathbf{x}}_- := \begin{pmatrix} \hat{q}_- \\ \hat{p}_- \end{pmatrix} = \frac{\hat{\mathbf{x}}_{s'} - \hat{\mathbf{x}}_{i'}}{\sqrt{2}}, \quad (157)$$

and

$$\hat{\mathbf{x}}_+ := \begin{pmatrix} \hat{q}_+ \\ \hat{p}_+ \end{pmatrix} = \frac{\hat{\mathbf{x}}_{s'} + \hat{\mathbf{x}}_{i'}}{\sqrt{2}}. \quad (158)$$

Here the ‘‘EPR quadratures’’  $\{\hat{q}_-, \hat{p}_+\}$  are measured by using two homodyne detectors. The corresponding outcome  $\{q_-, p_+\}$  is classically processed via a  $\chi^2$ -test, whose output is the value of the bit stored in the memory cell. In general, for arbitrary bandwidth  $M \geq 1$ , we have  $M$  identical copies  $|\xi\rangle\langle\xi|^{\otimes M}$  at the input and, therefore,

$2M$  output variables  $\{q_-, p_+\}^M$  which are processed by the  $\chi^2$ -test.

Let us analyze the detection process in detail in order to derive the error-probability which affects the decoding. First of all we can easily verify that the two classical outputs,  $q_-$  and  $p_+$ , are identical Gaussian variables, so that we can simply use  $z$  to denote  $q_-$  or  $p_+$ . Clearly the Gaussian variable  $z$  is tested two times for each single-copy state  $|\xi\rangle\langle\xi|$  and, therefore,  $2M$  times during the reading time of the logical bit. This variable has zero mean and variance  $V = V(u)$  which is conditioned to the value of the stored bit  $u = 0, 1$ . Explicitly, we have

$$V(u) = \frac{1}{2} [r_u(\mu + \varepsilon) + (1 - r_u)\beta + \mu + 3\varepsilon - 2\sqrt{r_u(\mu^2 - 1)}], \quad (159)$$

where  $r_u$  is the conditional reflectivity of the cell,  $\mu := 2n_s + 1$  is the variance associated with the signal-mode,  $\beta := 2\bar{n} + 1$  is the noise-variance of the external thermal bath, and  $\varepsilon$  is the noise-variance of the internal thermal channel. It is clear that the decoding of the logical bit  $u$  corresponds to the statistical discrimination between two variances  $V(0)$  and  $V(1)$ . In other words, the variable  $z$  is subject to the hypothesis test

$$\begin{cases} H_0 (u = 0) : V = V(0), \\ H_1 (u = 1) : V = V(1). \end{cases} \quad (160)$$

It is easy to show that  $V$  of Eq. (159) is a decreasing function of the reflectivity  $r_u$  as long as

$$r_u < \frac{\mu^2 - 1}{(\varepsilon - \beta + \mu)^2}, \quad (161)$$

which is always true in the regime considered here (i.e.,  $\varepsilon$  small and  $\beta$  close to 1). This means that  $r_0 < r_1$  implies  $V(0) > V(1)$ , which makes Eq. (160) a one-tailed test. Equivalently, we can introduce the normalized variable

$$z' := \frac{z}{\sqrt{V(1)}}, \quad (162)$$

with zero mean and variance  $V'(u) = V(u)/V(1)$ , and replace Eq. (160) with the one-tailed test

$$\begin{cases} H_0 : V' = 1 + \Sigma, \\ H_1 : V' = 1. \end{cases} \quad (163)$$

where

$$\Sigma := \frac{V(0) - V(1)}{V(1)} > 0. \quad (164)$$

Thus, assuming  $r_0 < r_1$ , the decoding of the logical bit is equivalent to the statistical discrimination between the two hypotheses in Eq. (163), i.e.,  $V' > 1$  and  $V' = 1$ .

For arbitrary bandwidth  $M$ , we collect  $2M$  independent outcomes  $\{z_1, \dots, z_{2M}\}$  and we construct the  $\chi^2$ -variable

$$\theta := \sum_{k=1}^{2M} (z'_k)^2. \quad (165)$$

Then, we select one of the two hypotheses according to the following rule

$$\begin{cases} \text{Accept } H_0 \Leftrightarrow \theta \geq \mathcal{Q}_{1-\varphi}^{2M-1}, \\ \text{Accept } H_1 \Leftrightarrow \theta < \mathcal{Q}_{1-\varphi}^{2M-1}. \end{cases} \quad (166)$$

where  $\mathcal{Q}_{1-\varphi}^{2M-1}$  is the  $(1-\varphi)^{th}$  quantile of the  $\chi^2$  distribution with  $2M-1$  degrees of freedom. Here the quantity  $\varphi$  represents the significance level of the test, corresponding to the asymptotic probability of wrongly rejecting the hypothesis  $H_1$ , i.e.,

$$\varphi = \lim_{M \rightarrow \infty} P(H_0|H_1). \quad (167)$$

This quantity must be fixed and its value characterizes the test. In particular, for finite  $M$ , there will be an optimal value of  $\varphi$  which maximizes the performance of the test.

Let us explicitly compute the error probability affecting the classical test. For arbitrary variance  $V'$ , the  $\chi^2$  distribution with  $2M-1$  degrees of freedom is equal to

$$P_{M,V'}(\theta) = \frac{\theta^{M-1} \exp\left(-\frac{\theta}{2V'}\right)}{(2V')^M \Gamma(M)}, \quad (168)$$

where  $\Gamma(x)$  is the Gamma function. The probability of finding  $\theta$  bigger than  $t$  is given by the integral

$$I(M, V', t) := \int_t^{+\infty} P_{M,V'}(\theta) d\theta = \frac{\Gamma\left(M, \frac{t}{2V'}\right)}{\Gamma(M)}. \quad (169)$$

where  $\Gamma(x, y)$  is the incomplete Gamma function. Thus, given  $H_1$  (i.e.,  $V' = 1$ ) the probability of accepting  $H_0$  (i.e.,  $\theta \geq \mathcal{Q}_{1-\varphi}^{2M-1}$ ) is given by

$$P(H_0|H_1) = I(M, 1, \mathcal{Q}_{1-\varphi}^{2M-1}). \quad (170)$$

By contrast, given  $H_0$  (i.e.,  $V' = 1 + \Sigma$ ) the probability of accepting  $H_1$  (i.e.,  $\theta < \mathcal{Q}_{1-\varphi}^{2M-1}$ ) is given by

$$P(H_1|H_0) = 1 - I(M, 1 + \Sigma, \mathcal{Q}_{1-\varphi}^{2M-1}). \quad (171)$$

From Eqs. (170) and (171) we compute the error probability affecting the test, which is given by

$$\begin{aligned} P_{test} &:= \frac{1}{2} [P(H_0|H_1) + P(H_1|H_0)] \\ &= \frac{1}{2} + \frac{1}{2} [I(M, 1, \mathcal{Q}_{1-\varphi}^{2M-1}) - I(M, 1 + \Sigma, \mathcal{Q}_{1-\varphi}^{2M-1})] \\ &= P_{test}(r_0, r_1, N, M, \bar{n}, \varepsilon, \varphi). \end{aligned} \quad (172)$$

Clearly this quantity depends on all the parameters of the model, i.e., memory reflectivities  $\{r_0, r_1\}$ , energy and bandwidth of the signal  $\{N, M\}$ , levels of noise  $\{\bar{n}, \varepsilon\}$  and significance level of the test  $\varphi$ . This error probability must be compared with the classical discrimination bound  $\mathcal{C}$ . For simplicity let us first consider the pure-loss model ( $\bar{n} = \varepsilon = 0$ ). In this case  $P_{test} = P_{test}(r_0, r_1, N, M, \varphi)$  must be compared with  $\mathcal{C} = \mathcal{C}(r_0, r_1, N)$  of Eq. (91). Then, for given memory  $\{r_0, r_1\}$  and signal-energy  $N$ , we have that quantum reading is superior if we find a bandwidth  $M$  and a significance level  $\varphi$  such that  $P_{test} < \mathcal{C}$ . This is equivalent to prove the positivity of the (sub-optimal) information gain

$$G_{test} = 1 - H(P_{test}) - [1 - H(\mathcal{C})], \quad (173)$$

which provides a lowerbound to the number of bits per cell which are gained by quantum reading over any classical strategy. In Fig. 4(left) we optimize  $G_{test}$  over  $M$  and  $\varphi$  for an ideal memory in the few-photon regime. Remarkably, we can find an area where  $G_{test} > 0.6$  bits per cell.

Then, let us consider the thermal-loss model, with  $\bar{n} = \varepsilon = 10^{-5}$ . In this case,  $P_{test} = P_{test}(r_0, r_1, N, M, \bar{n}, \varepsilon, \varphi)$  must be compared with  $\mathcal{C} = \mathcal{C}(r_0, r_1, N, M^*, \bar{n}, \varepsilon)$  where the value of  $M^*$  is high enough to include all the classical transmitters which are meaningful for the model (here we take  $M^* = 10^6$ ). In Fig. 4(right), we consider a memory with  $r_0 = 0.85$  and  $r_1 = 0.95$  (high-reflectivity regime), which is illuminated by a signal with  $N = 100$  (few-photon regime). The numerical optimization over  $M$  and  $\varphi$  shows an area where  $G_{test} > 0.5$  bits per cell.

Thus, the remarkable advantages of quantum reading are still evident when the optimal Helstrom's POVM is replaced by a sub-optimal receiver, consisting of a Bell measurement followed by a suitable classical post-processing. This sub-optimal receiver can be easily realized in today's quantum optics labs, thus making quantum reading a technique within the catch of current technology.

[1] M. A. Nielsen, and I. L. Chuang, *Quantum Computation and Quantum Information* (Cambridge University Press, Cambridge, 2000).

[2] S. L. Braunstein, and P. van Loock, *Rev. Mod. Phys.* **77**, 513 (2005).

[3] For every  $K$ -mode bosonic state  $\rho$ , we can write the  $\mathcal{P}$ -representation  $\rho = \int d^{2K} \alpha \mathcal{P}(\alpha) |\alpha\rangle \langle \alpha|$ , where  $\mathcal{P}(\alpha)$  is normalized to 1 and  $|\alpha\rangle \langle \alpha|$  is a generic multimode coherent state. By definition,  $\rho$  is called "classical" ("non-classical") if  $\mathcal{P}(\alpha)$  is positive (non-positive) [4]. For a

- classical state,  $\mathcal{P}(\alpha)$  represents a probability distribution (implying separability).
- [4] E. C. G. Sudarshan, Phys. Rev. Lett. **10**, 277 (1963); R. J. Glauber, Phys. Rev. **131**, 2766 (1963).
- [5] A. Einstein, B. Podolsky, and N. Rosen, Phys. Rev. **47**, 777 (1935).
- [6] For two bosonic modes,  $A$  and  $B$ , with quadratures  $\hat{q}_A$ ,  $\hat{p}_A$ ,  $\hat{q}_B$  and  $\hat{p}_B$ , one can define the two operators  $\hat{q}_- := (\hat{q}_A - \hat{q}_B)/\sqrt{2}$  (relative position) and  $\hat{p}_+ := (\hat{p}_A + \hat{p}_B)/\sqrt{2}$  (total momentum). Then, the system has EPR correlations (in these operators) if  $V(\hat{q}_-) + V(\hat{p}_+) < 2\nu_0$ , where  $V(\cdot)$  is the variance, and  $\nu_0$  is the standard quantum limit ( $\nu_0 = 1$  in this paper.) Note that a bosonic system with EPR correlations is entangled, but the contrary is not necessarily true. In today's quantum optics labs, the EPR correlations represent the standard type of continuous variable entanglement. These correlations are usually generated via spontaneous parametric down conversion.
- [7] H. P. Yuen, and R. Nair, Phys. Rev. A **80**, 023816 (2009).
- [8] S.-H. Tan *et al.*, Phys. Rev. Lett. **101**, 253601 (2008); S. Lloyd, Science **321**, 1463 (2008).
- [9] S. Guha and B. Erkmen, Phys. Rev. A **80**, 052310 (2009).
- [10] J. H. Shapiro and S. Lloyd, arXiv:0902.0986; J. H. Shapiro, arXiv:0903.3150; *ibid.*, arXiv:0904.2490.
- [11] A. R. Usha Devi and A. K. Rajagopal, Phys. Rev. A **79**, 062320 (2009).
- [12] Note that an example of classical transmitter is the coherent-state transmitter  $T(M, 0, \rho)$ , with no idlers and  $\rho = \otimes_{k=1}^M |\alpha_k\rangle \langle \alpha_k|$  a tensor product of coherent states.
- [13] K. M. R. Audenaert *et al.*, Phys. Rev. Lett. **98**, 160501 (2007); J. Calsamiglia *et al.*, Phys. Rev. A **77**, 032311 (2008).
- [14] S. Pirandola and S. Lloyd, Phys. Rev. A **78**, 012331 (2008).
- [15]  $G > 0$  is a sufficient condition for the superiority of quantum reading.  $G = 1$  corresponds to the singular case where only quantum light can retrieve information.
- [16] For increasing  $N$ , the black region in Fig. 2 tends to shrink towards the bisector  $r_0 = r_1$ , but, at the same time,  $G$  decreases to zero almost everywhere.
- [17] C. F. Bohren, and D. Huffman, *Absorption and scattering of light by small particles* (John Wiley, New York, 1983).
- [18] C.W. Helstrom, *Quantum detection and estimation theory* (Academic Press, New York, 1976).
- [19] In an alternative optical implementation, the signal can be seen as a train of  $M$  quasi-monochromatic pulses, each one with carrier frequency  $\omega$  and duration  $\tau \simeq W^{-1}$ .
- [20] A single-layer CD with speed 1X (i.e., 500 rpm) has data-transfer rate of 1.2 Mbit/s. This data is read by a laser diode at 780 nm and power  $\approx 5$  mW, therefore irradiating about 5 nJ per bit. A higher-speed CD needs a laser with proportionally more power, in such a way that at least 1 nJ per bit is irradiated, corresponding to  $N \simeq 10^{10}$  photons per bit.
- [21] J. Taylor, M. R. Johnson, and C. G. Crawford, *DVD demystified* (McGraw-Hill, 2005). See also wikipedia.
- [22] Clearly, the higher is the carrier frequency the smaller is the cell that can be resolved.
- [23] M. Fiorentino *et al.*, Opt. Express **15**, 7479 (2007).
- [24] A. Hayat *et al.*, Nature Photonics **2**, 256 (2008).
- [25] In standard CD-R and DVD-R media, the data is recorded in internal layers of organic dye (e.g., Azo, Cyanine, or Phthalocyanine). The dye polymer darkens when heated by a high-power laser, with the result of causing less reflection from the metallic layer underneath (dye-sublimation [21]).
- [26] [http://en.wikipedia.org/wiki/UV\\_degradation](http://en.wikipedia.org/wiki/UV_degradation).
- [27] With the notation  $[\hat{\mathbf{x}}, \hat{\mathbf{x}}^T]$  we mean a matrix with entries  $[\hat{\mathbf{x}}_i, \hat{\mathbf{x}}_j]$ , where  $i, j = 1, \dots, 2n$ . Analogously,  $\{\hat{\mathbf{x}}, \hat{\mathbf{x}}^T\}$  is a matrix with entries  $\{\hat{\mathbf{x}}_i, \hat{\mathbf{x}}_j\}$ .
- [28] A. Ferraro, S. Olivares, and M. Paris, *Gaussian states in quantum information*, ISBN 88-7088-483-X (Biliopolis, Napoli, 2005).
- [29] J. Eisert and M. B. Plenio, Int. J. Quant. Inf. **1**, 479 (2003).
- [30] S. L. Braunstein and A. K. Pati, *Quantum Information Theory with Continuous Variables*, (Kluwer Academic, Dordrecht, 2003).
- [31] R. Simon, N. Mukunda, and B. Dutta, Phys. Rev. A **49**, 1567 (1994).
- [32] S. Pirandola, A. Serafini, and S. Lloyd, Phys. Rev. A **79**, 052327 (2009).
- [33] G. Milburn and D. Walls, *Quantum Optics* (Springer 1994).
- [34] A. S. Holevo, Prob. of Inf. Transm. **43**, 1 (2007).
- [35] S. Pirandola, S. L. Braunstein, and S. Lloyd, Phys. Rev. Lett. **101**, 200504 (2008).
- [36] A. Serafini, J. Eisert, and M. M. Wolf, Phys. Rev. A **71**, 012320 (2005).
- [37] Note that in our Letter we use the short-hand notation  $P_{err}(T) := P_{err}(\mathcal{E}_0 \neq \mathcal{E}_1|T)$ .
- [38] In other words,  $\Pi(\gamma_+)$  projects onto the subspace spanned by the eigenstates of  $\gamma$  with positive eigenvalues.
- [39] We use the notation  $\int d^2M \alpha = \int d^2\alpha_1 \dots \int d^2\alpha_M$ .
- [40] C. A. Fuchs and J. V. de Graaf, IEEE Trans. Inf. Theory **45**, 1216 (1999).
- [41] C. Fuchs, PhD thesis (Univ. of New Mexico, Albuquerque, 1995).
- [42] H. Scutaru, J. Phys. A **31**, 3659 (1998).
- [43] Jensen's inequality states that, for every random variable  $\mathbf{x}$ , with values in  $\mathbb{R}^M$  and expectation value  $\langle \mathbf{x} \rangle$ , and for any concave function  $f : \mathbb{R}^M \rightarrow \mathbb{R}$ , we have  $\langle f(\mathbf{x}) \rangle \leq f(\langle \mathbf{x} \rangle)$  (the inequality is reversed for convex functions). More in general, the inequality holds for random variables and concave functions which are defined in measurable subsets  $\Omega \subset \mathbb{R}^M$ .
- [44] Numerical investigations can also be performed by using the simpler quantity

$$G' := 1 - H(\mathcal{B}) - [1 - H(\mathcal{C})] \leq G,$$

which is based on the quantum Battacharyya bound.